Transition Prediction and Modeling in External Flows Using RANS-based CFD Codes

Andreas Krumbein, Normann Krimmelbein, Cornelia Grabe

Deutsches Zentrum für Luft- und Raumfahrt
Institut für Aerodynamik und Strömungstechnik
$C^2A^2S^2E$ Center for Computer Applications in AeroSpace Science and Engineering

Deutsches Zentrum für Luft- und Raumfahrt e.V. in der Helmholtz-Gemeinschaft

Overview
Transition Prediction in RANS-based CFD of External Flows

- Introduction
- Transition Prediction using Local, Linear Stability and the e^N method
  - Structure of the Prediction Approach
  - Test Cases & Computational Results
- The γ-$Re_{\theta,t}$ Transport Equation Model
  - The Original Model
  - Test Cases & Computational Results
  - Extension to Three-dimensional Flows
- Conclusion & Outlook

Introduction
Transition Prediction in RANS-based CFD of External Flows

Current status of transition prediction in RANS solvers

- RANS solvers have become a standard approach for the design and the aerodynamic analysis of aerodynamic configurations.
- Requirement from Aircraft Industry and Research for a long time:
  - RANS solver with integrated general transition prediction functionality
  - Automatic: no intervention of the user
  - Autonomous: as little additional information as possible
- Major aims:
  - Reduction of modeling based uncertainties
  - Improvement of simulation accuracy
- Accuracy of results from fully turbulent computations or from computations with prescribed transition often not satisfactory (e.g. suppression of separation)
- Exploitation of the full potential of advanced turbulence models
- Most important, at present, improved simulation of the interaction between transition locations and separation, especially for high-lift configurations.

Introduction
Transition Prediction in RANS-based CFD of External Flows

Current status of transition prediction in RANS solvers

$M = 0.2$, $Re = 2.3 \times 10^6$, $\alpha = -4.0°$, $i_{HTP} = 4°$

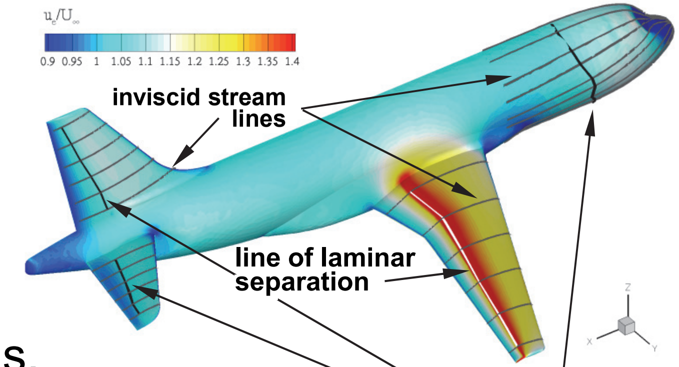

- Incorporated transition prediction has become a *state-of-the-art* technique for various RANS codes in the last years.
- Details of the concepts are different. They have in common that they are able to be applied to complex geometries: multi-element configurations, full aircraft, high-lift configurations, wind turbines, fuselages, etc.
- Much development and validation work has been carried out and, today, the approaches have gained a high level of confidence.

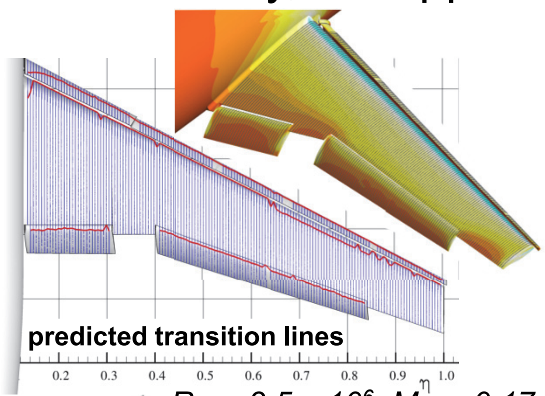

$Re = 3.5 \times 10^6$, $Ma = 0.17$

- Standard approaches of the transition prediction functionalities regularly used in aircraft industry.
- Currently, increasing use of advanced approaches at universities and research organizations.
- Growing computer capacities will allow for more complex geometries and more points.

Introduction
Transition Prediction in RANS-based CFD of External Flows

Currently most commonly used approaches for 3D RANS simulations

- RANS solver + laminar BL code + e^N database methods/empirical criteria
- RANS solver + laminar BL code + automated stability code + e^N methods
- RANS solver + + e^N database methods/empirical criteria
- RANS solver + + automated stability code + e^N methods
- RANS solver + + transition transport equation models

Introduction
Transition Prediction in RANS-based CFD of External Flows

Currently most commonly used approaches for 3D RANS simulations

- RANS solver + laminar BL code + e^N database methods/empirical criteria

- RANS solver + laminar BL code + automated stability code + e^N methods (1)
  $\rightarrow$ standard approach, industrial applications, standard grids can be used: only c_p

- RANS solver + + e^N database methods/empirical criteria

- RANS solver + + automated stability code + e^N methods (2)
  $\rightarrow$ advanced approach, accurate in regions where BL codes can not be applied

- RANS solver + + transition transport equation models (3)
  $\rightarrow$ γ-$Re_{\theta,t}$ model by Menter/Langtry works well and yields accurate results for streamwise transition
  $\rightarrow$ first promising results for CF at infinite swept wings: γ-$Re_{\theta,t}$-$Re_{\delta 2,t}$

Transition Prediction using the e^N method
Structure of the Prediction Approach – Process Chain

- RANS solvers:
  - DLR TAU code
  - DLR FLOWer code
- Transition prescription
- Automatic transition prediction
- 2D and 3D flows
- Parallel
- e^N-method (2 N-factor method)
- Various transition criteria
- External codes
  - Stability solver LILO (G. Schrauf)
  - Laminar boundary layer code COCO (G. Schrauf)

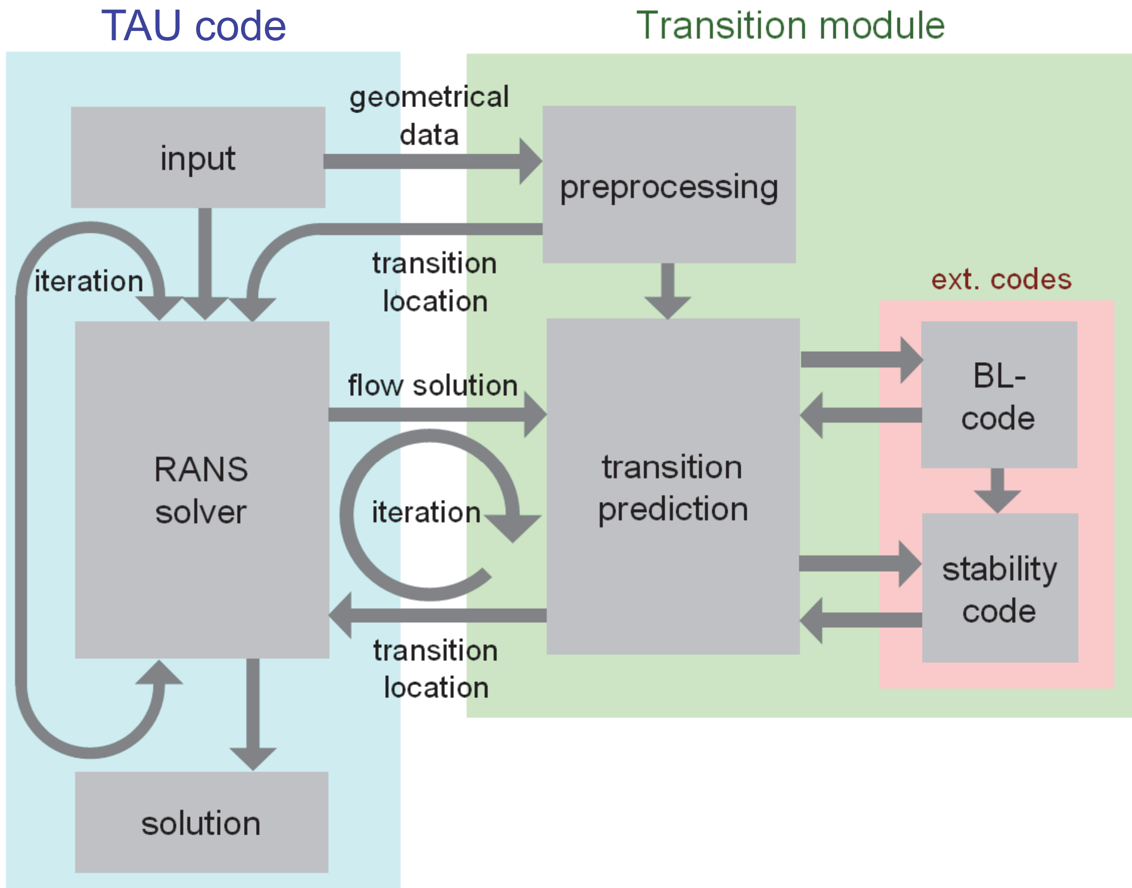

Transition Prediction using the e^N method
Structure of the Prediction Approach – Application in 3D

- Transition criteria need laminar boundary-layer data (integral values, velocity profiles)
- Two different approaches:
  - Navier-Stokes data
  - Laminar boundary-layer code
- Application of transition criteria along inviscid streamlines or approximations of streamlines
- Transition points form a polygonal line on a 3D surface of the geometry, the transition line.
- Criteria, for example, AHD, C1, Michel, e^N-method (stability code, envelope methods)

e^N-method with stability solver LILO

- 2 *N*-factors in 3D: TS and CF
- Different strategies
  - Prescribe frequency and propagation direction (TS)
  - Prescribe frequency and wavelength (CF)
- Integration path in 3D:
  - Energy transport of a wave represented by the group velocity
  - Group velocity direction can be taken as amplification direction
  - Group velocity trajectory can be approximated by inviscid streamline

$$N = \ln(A/A_0)_{wave} = \int_{x_0}^{x} \sigma \, dx$$

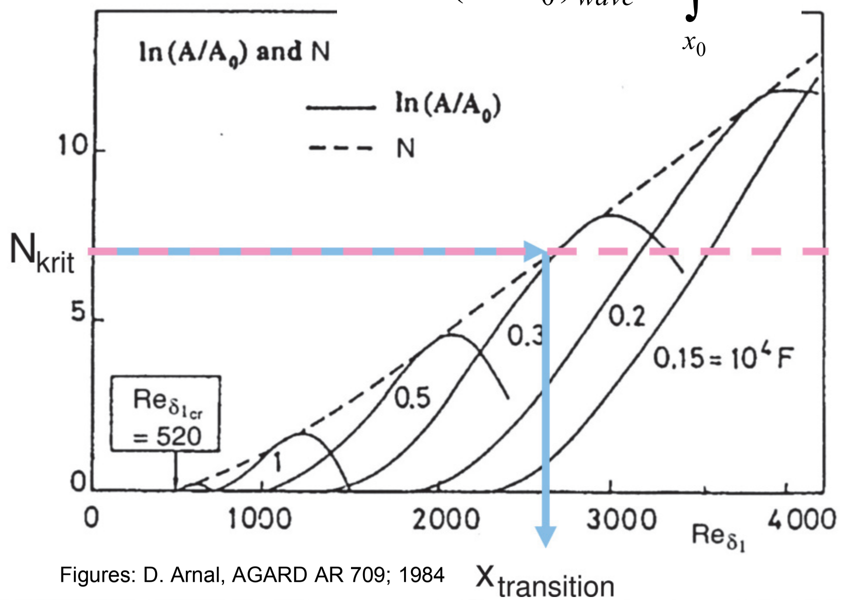

Figures: D. Arnal, AGARD AR 709; 1984

Transition Prediction using the e^N method

Structure of the Prediction Approach

Application in 3D

The stability boundary

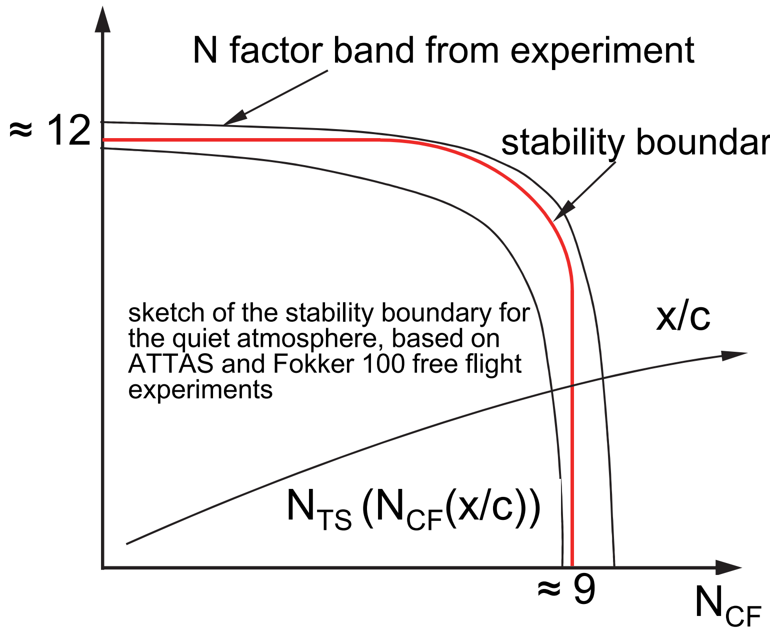

ELFIN II tests

S1Ma wind tunnel

incompressible analysis for transonic flow

G. Schrauf: *"Large-Scale Laminar-Flow Tests Evaluated with Linear Stability Theory"*, JoA, Vol. 41, No. 2, 2004, 224-230

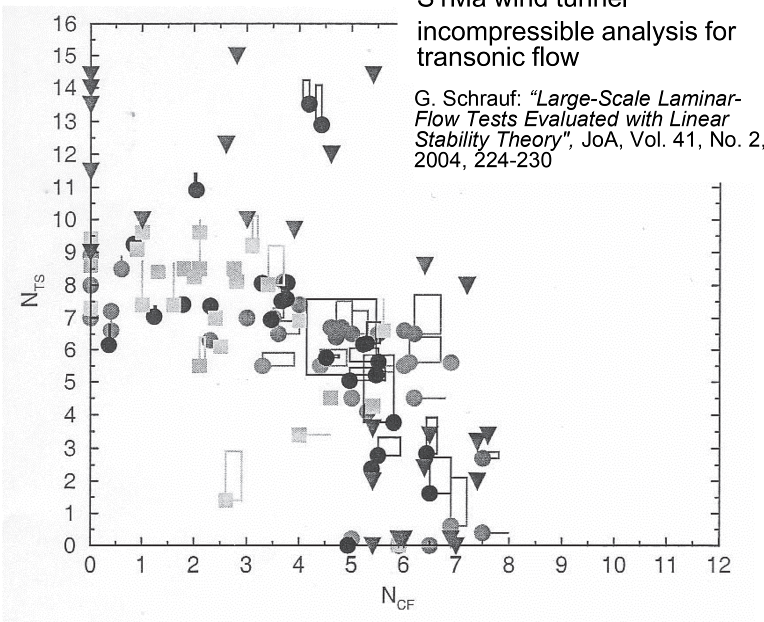

prolate spheroid in NWG

(LSWT Göttingen; Kreplin, Vollmers, Meier)

H. W. Stock: *"e^N Transition Prediction in Three-Dimensional Boundary Layers on Inclined Prolate Spheroids"*, AIAAJ, Vol. 44, No. 1, 2006, 108-118

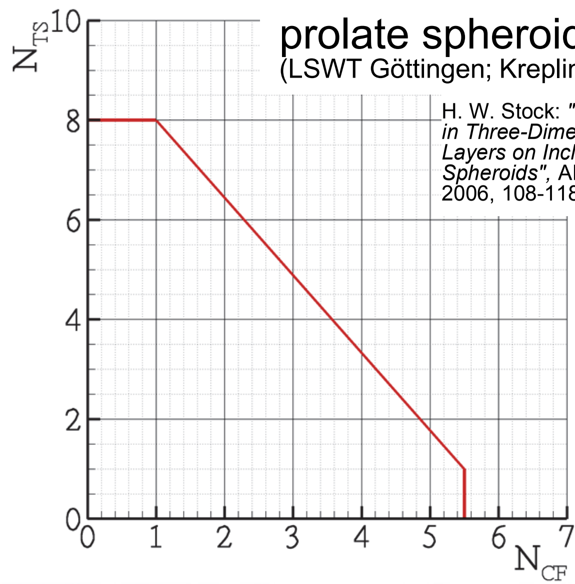

- Problem for wind tunnels: For most wind tunnels only very limited or no information available which could be used for the validation of transition prediction methods or models → reliable Tu_∞, N factors, transition locations, skin friction distributions, sufficient information on measurement techniques, error bands ⇒ *high uncertainty level*

Transition Prediction using the e^N method

Structure of the Prediction Approach – Calculation of BL data

- **Internal BL approach**
- Boundary-layer data from Navier-Stokes solution
- Projection of BL edge velocities onto surface
- Integration of edge velocities
- Inviscid streamlines
- Moderate (TS) / high (CF) grid resolution
- Wide range of applications

- **External BL approach**
- Boundary-layer data from BL code COCO (2.75D)
- “Line-in-flight” cuts
- Pressure distribution along cuts
- Length of inviscid streamline from BL-edge velocities
- Low grid resolution
- Limited to high aspect ratio wings

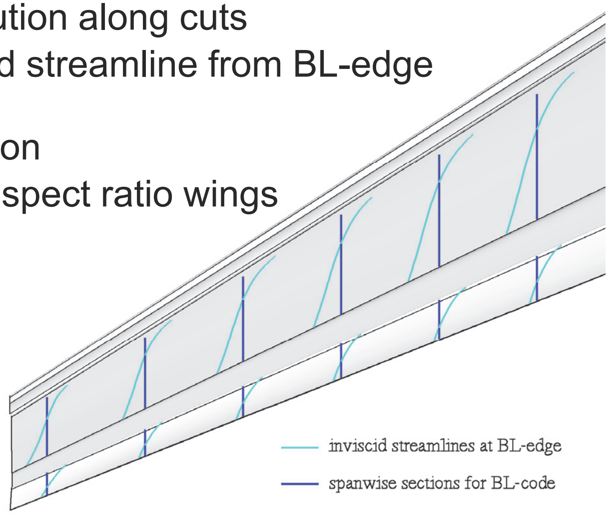

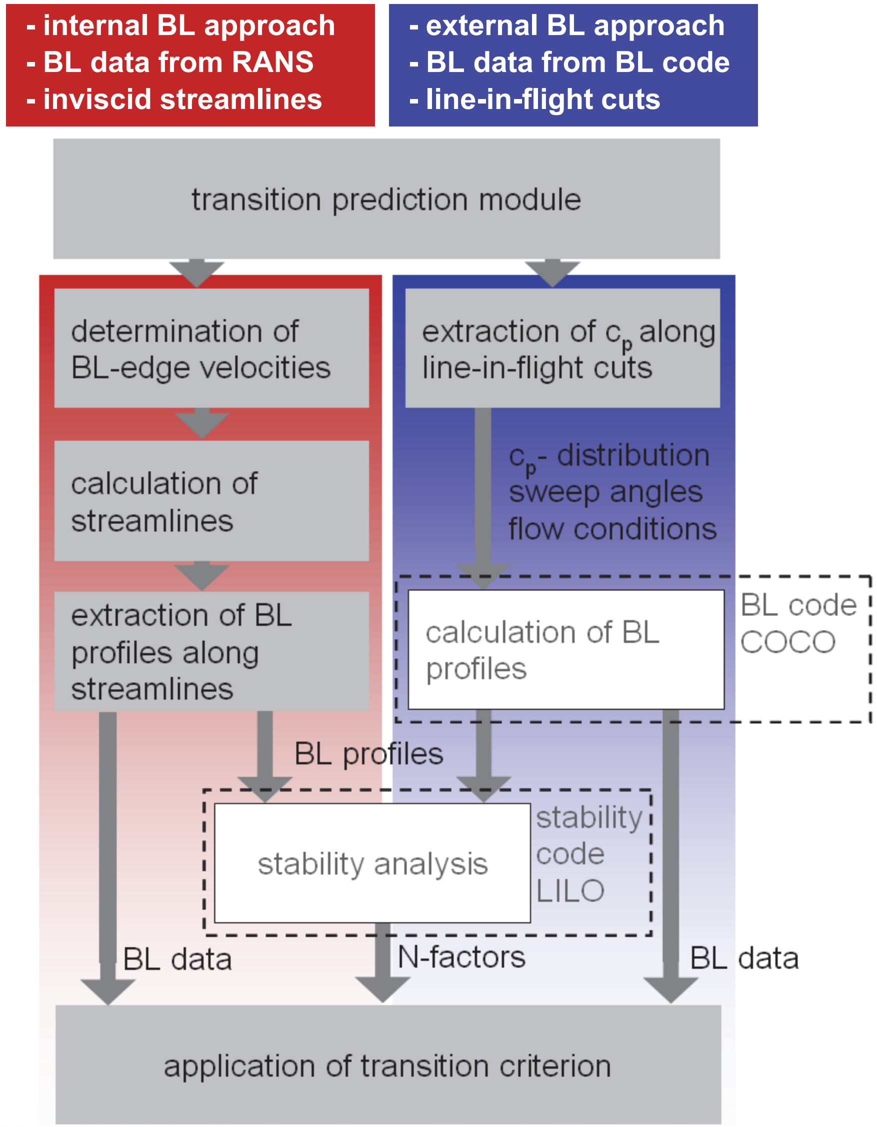

Transition Prediction using the e^N method
Structure of the Prediction Approach – Transition Lines

Mapping of transition point information into the computational grid

- **Surface information**
  - Predicted transition line is polygonal line on the surface of the configuration.
  - Linear interpolation for all surface points between two points of a transition line.
  - All points upstream of the transition line are flagged "laminar": $\gamma(P_s) = 0$.
  - All other points are flagged "turbulent": $\gamma(P_s) = 1$.

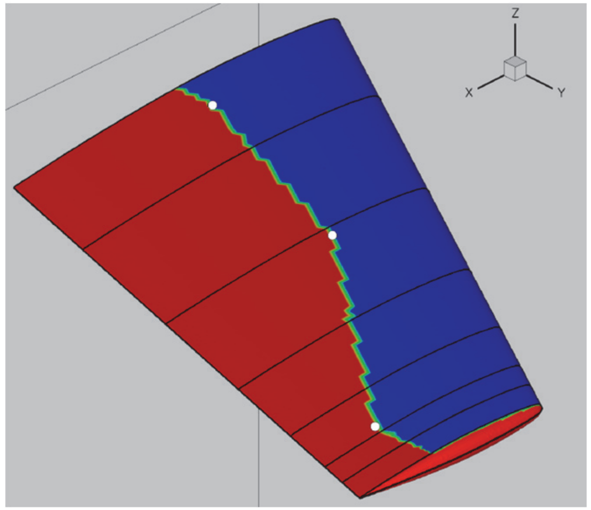

- **Field information**
  - Every field point knows its distance to the nearest solid wall and its nearest surface point.
  - A crude approximation of the wall-normal extension of the laminar boundary layer is done by generating a laminar zone near the wall.

Transition Prediction using the e^N method

Structure of the Prediction Approach – Laminar Zones

Mapping of transition point information into the computational grid

- An appropriate wall normal distance d_{lam} for each element of the configuration must be prescribed by the user.

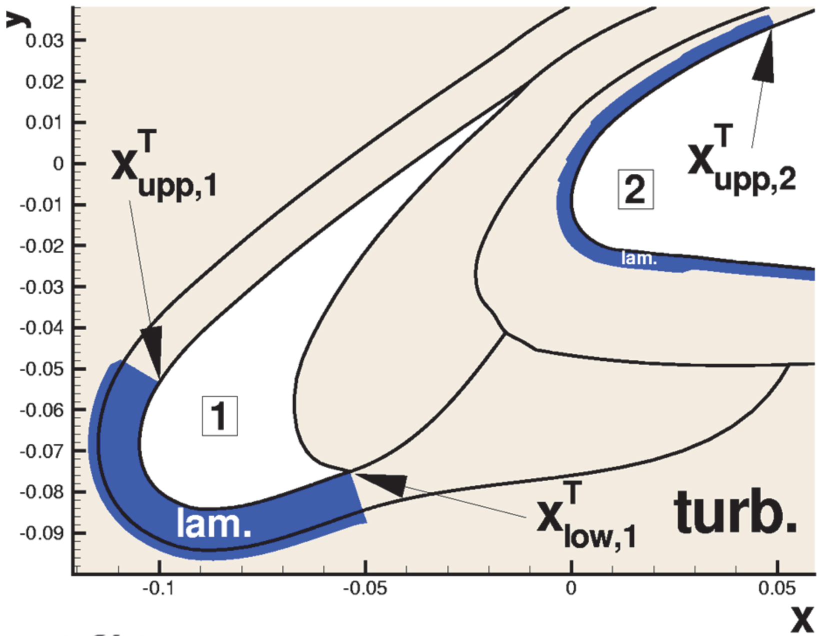

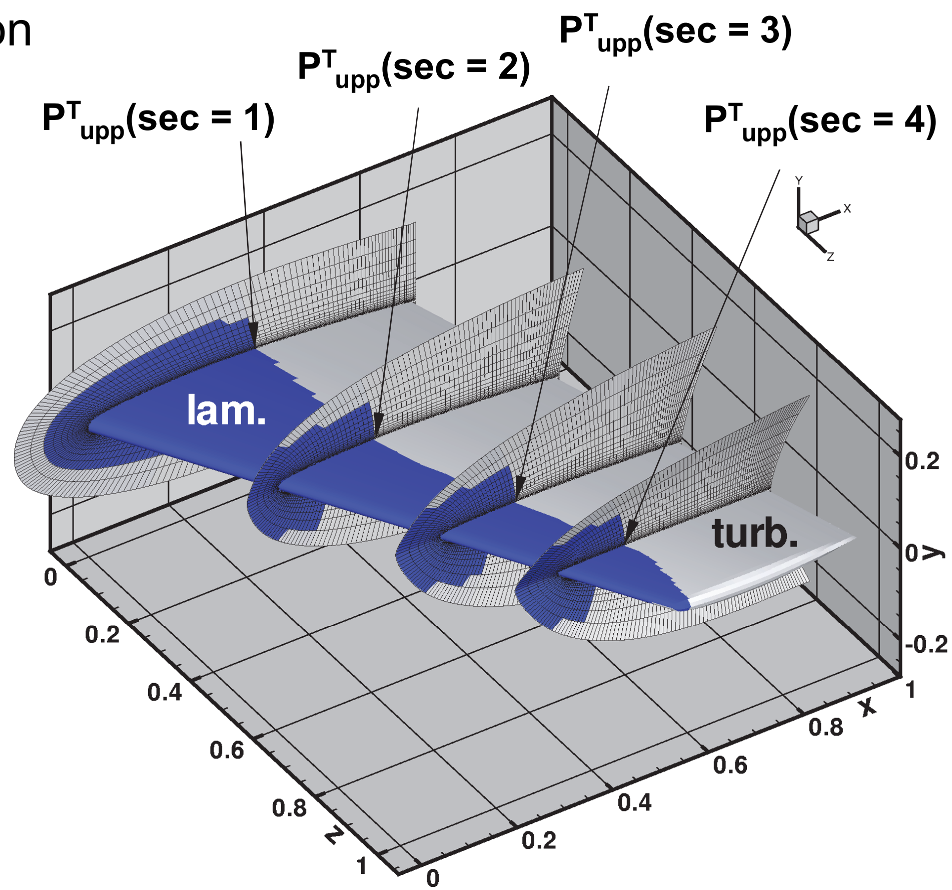

Transition Prediction using the e^N method
Structure of the Prediction Approach – Grid Point Treatment

Treatment of laminar and turbulent points

- **Laminar points**
  - The turbulence model is evaluated also in the laminar regions of the flow field.
  - The source term of any turbulence producing equation is limited for each laminar grid point: $S(P_{lam}) \leq 0$
- **Turbulent points**
  - The unchanged source term of the turbulence model is used.
  - Sudden switch from $\gamma = 0$ to $\gamma = 1$ from one to the next grid point ⇨ ‘point transition’
- **Coding**
  - $S^{code} = min\,[S, \gamma S]$
  - other approaches:
    - $S^{code} = \gamma S$: source term blanking
    - $S^{code} = min\,[P, c\,D^{\gamma}] - D$: with production limitation, sometimes used for k-ω models

Transition Prediction using the e^N method
Structure of the Prediction Approach – Parallelization

Parallelization of transition prediction approach

- Major issue in 3D transition prediction: capability to use parallel computation
- Main problem: non-local data is needed ⇨ high communication effort

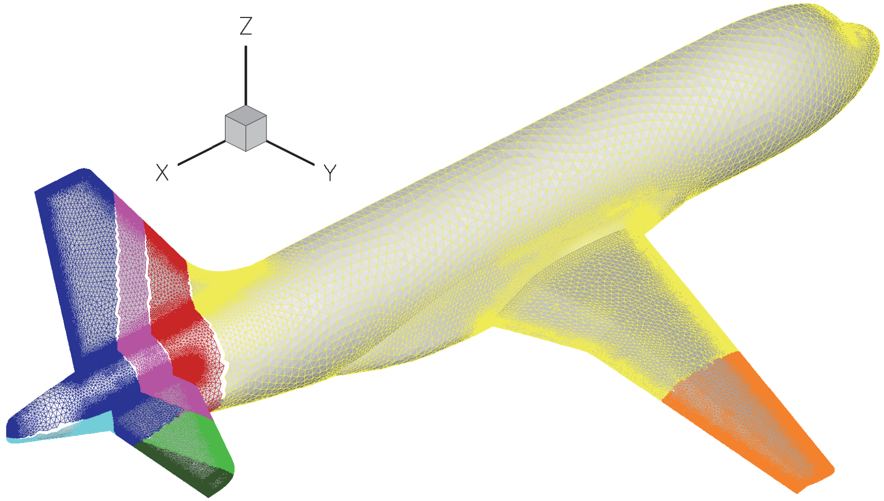

- parallel computation needed for
  - determination of wall normal grid points for the extraction of boundary-layer profiles
  - calculation of boundary-layer parameters and profiles
  - calculation of inviscid streamlines and line-in-flight cuts
  - parallel execution of external, sequential codes (COCO, LILO)

- parallel computation means: capable to use decomposed solutions, parallel transition analysis whenever possible and reasonable

Transition Prediction using the e^N method
Test Cases & Results – NLF(1)-0416

- external BL approach
- BL data from BL code
- line-in-flight cuts

Natural laminar airfoil

- $M = 0.1$, $Re = 4.0x10^6$, $Tu_\infty = 0.0003 \Rightarrow N_{TScrit} = 11.0$

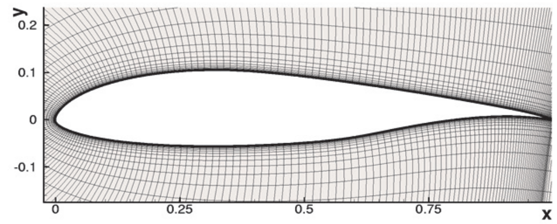

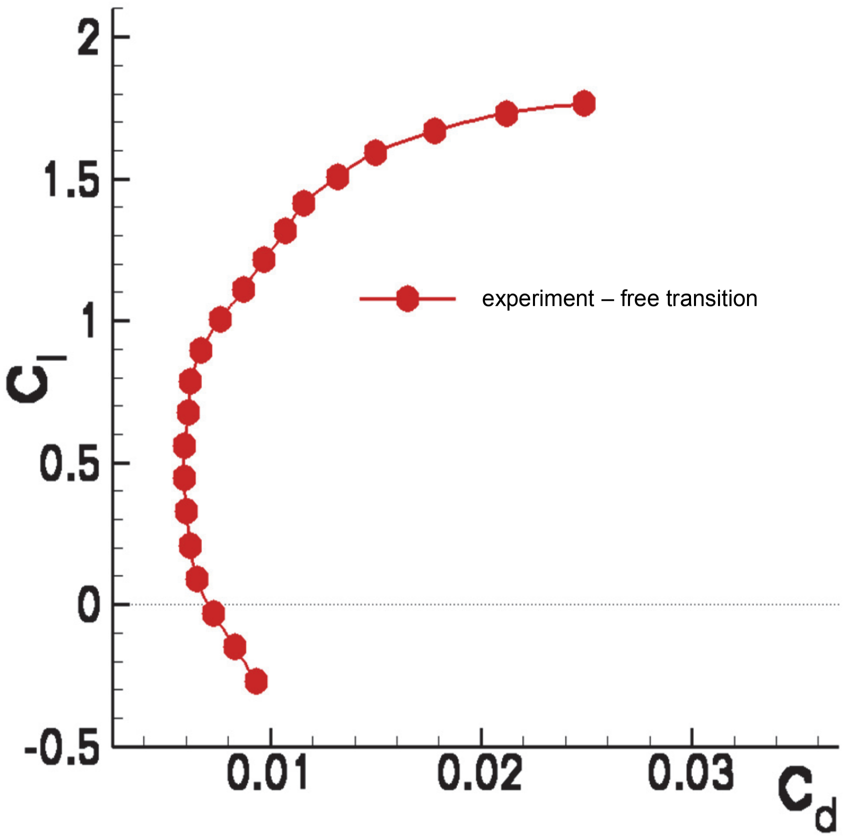

Force polars

Transition Prediction using the e^N method
Test Cases & Results – NLF(1)-0416

- external BL approach
- BL data from BL code
- line-in-flight cuts

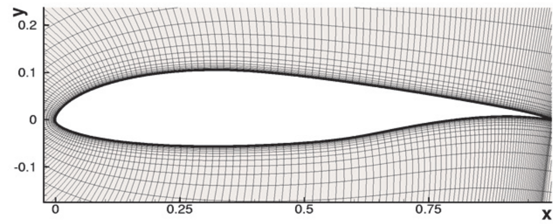

Natural laminar airfoil

- $M = 0.1$, $Re = 4.0x10^6$, $Tu_\infty = 0.0003 \Rightarrow N_{TScrit} = 11.0$

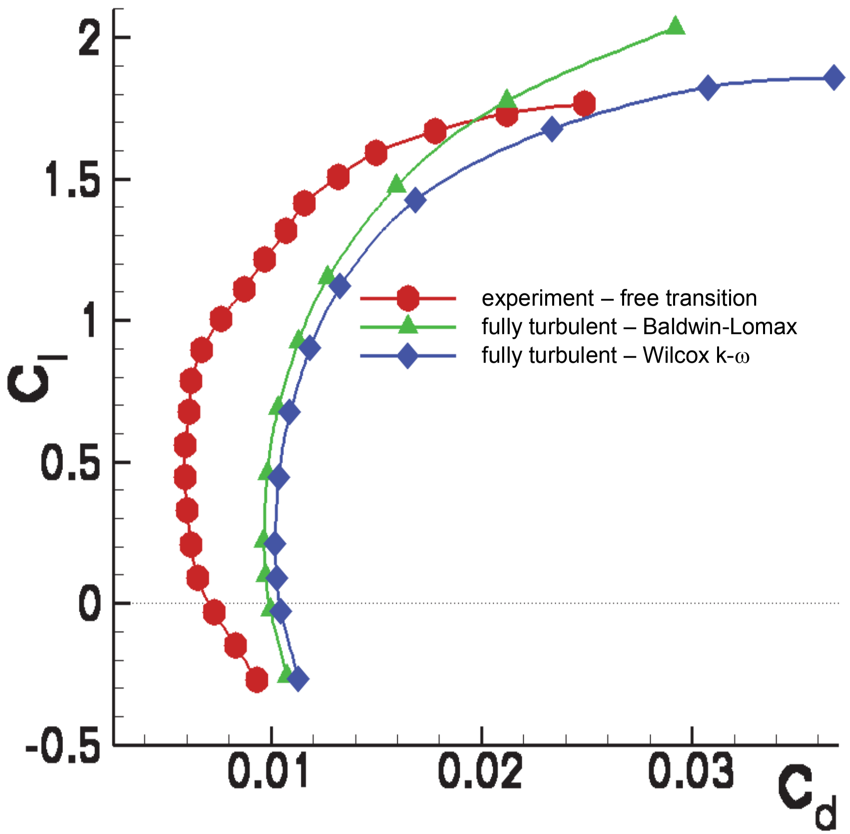

Force polars

Transition Prediction using the e^N method
Test Cases & Results – NLF(1)-0416

- external BL approach
- BL data from BL code
- line-in-flight cuts

Natural laminar airfoil

- $M = 0.1$, $Re = 4.0 \times 10^6$, $Tu_\infty = 0.0003 \Rightarrow N_{TScrit} = 11.0$

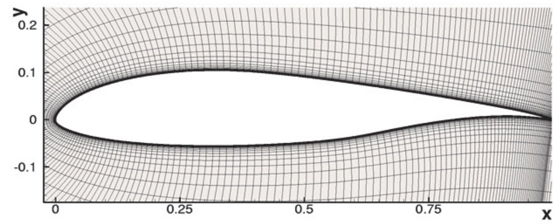

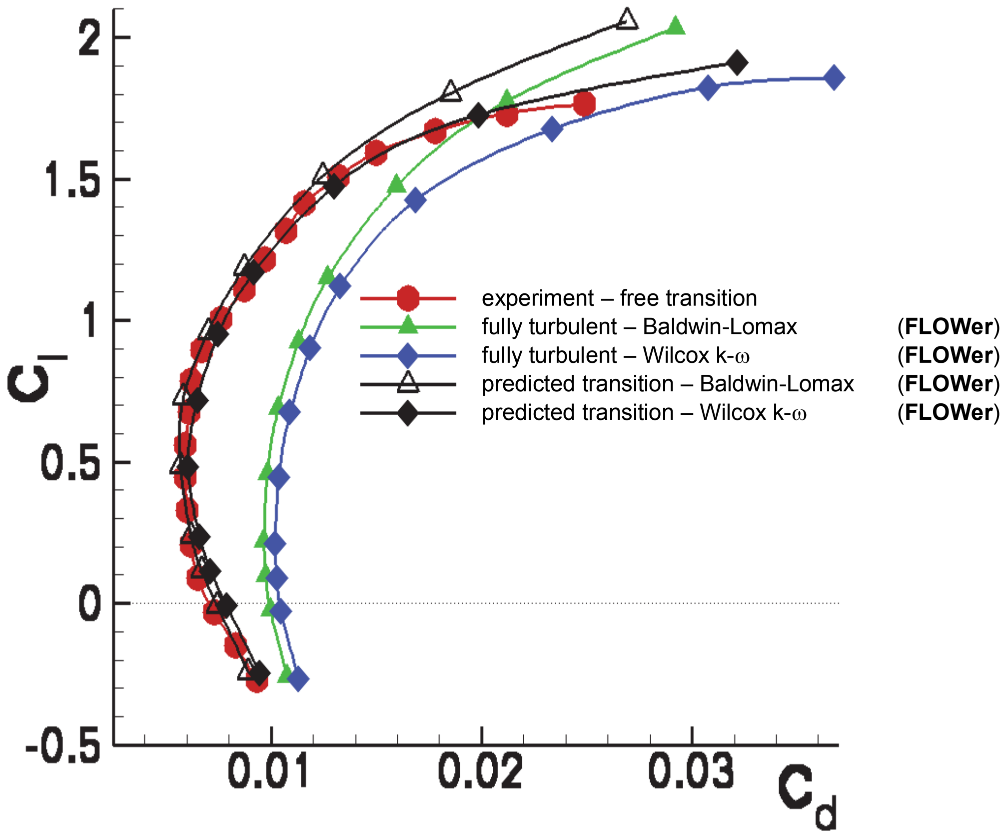

Force polars

Transition Prediction using the e^N method
Test Cases & Results – NLF(1)-0416

- external BL approach
- BL data from BL code
- line-in-flight cuts

Natural laminar airfoil

- $M = 0.1,\ Re = 4.0x10^6,\ Tu_\infty = 0.0003 \Rightarrow N_{TScrit} = 11.0$

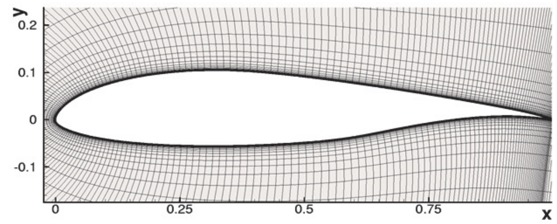

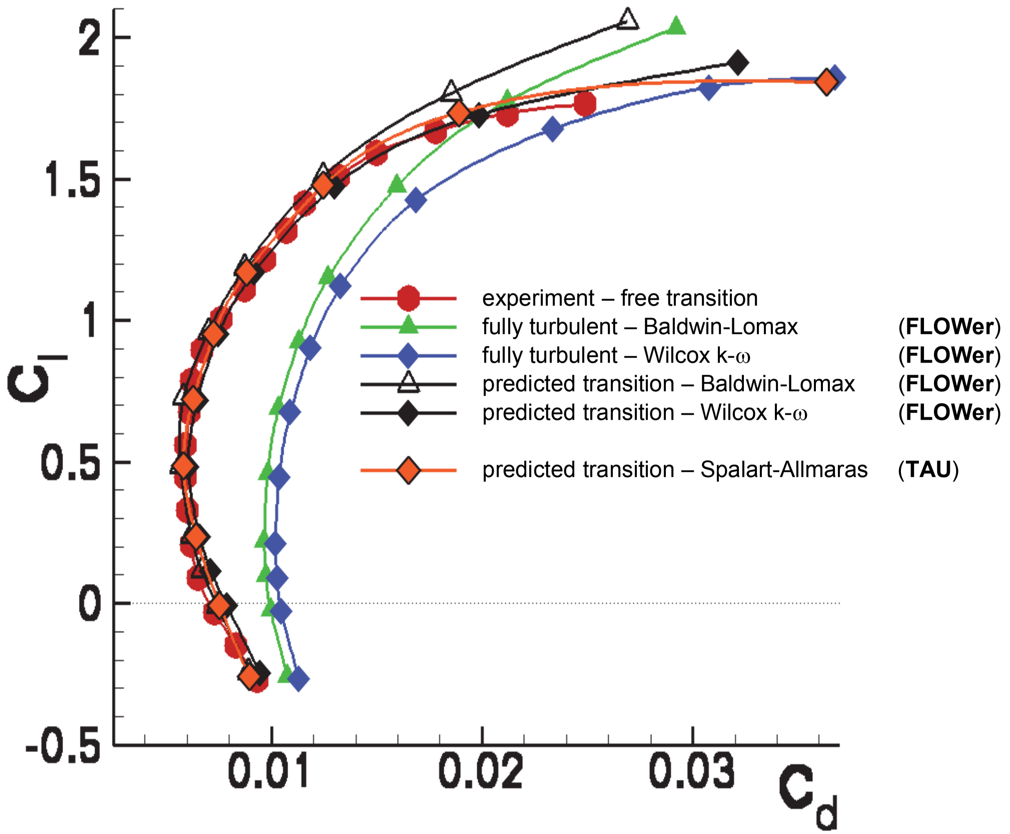

Force polars

Transition Prediction using the e^N method
Test Cases & Results – NLF(1)-0416

- external BL approach
- BL data from BL code
- line-in-flight cuts

Natural laminar airfoil

- $M = 0.1$, $Re = 4.0 \times 10^6$, $Tu_\infty = 0.0003 \Rightarrow N_{TScrit} = 11.0$

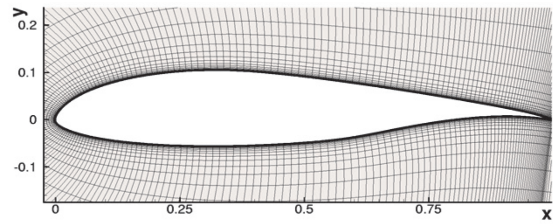

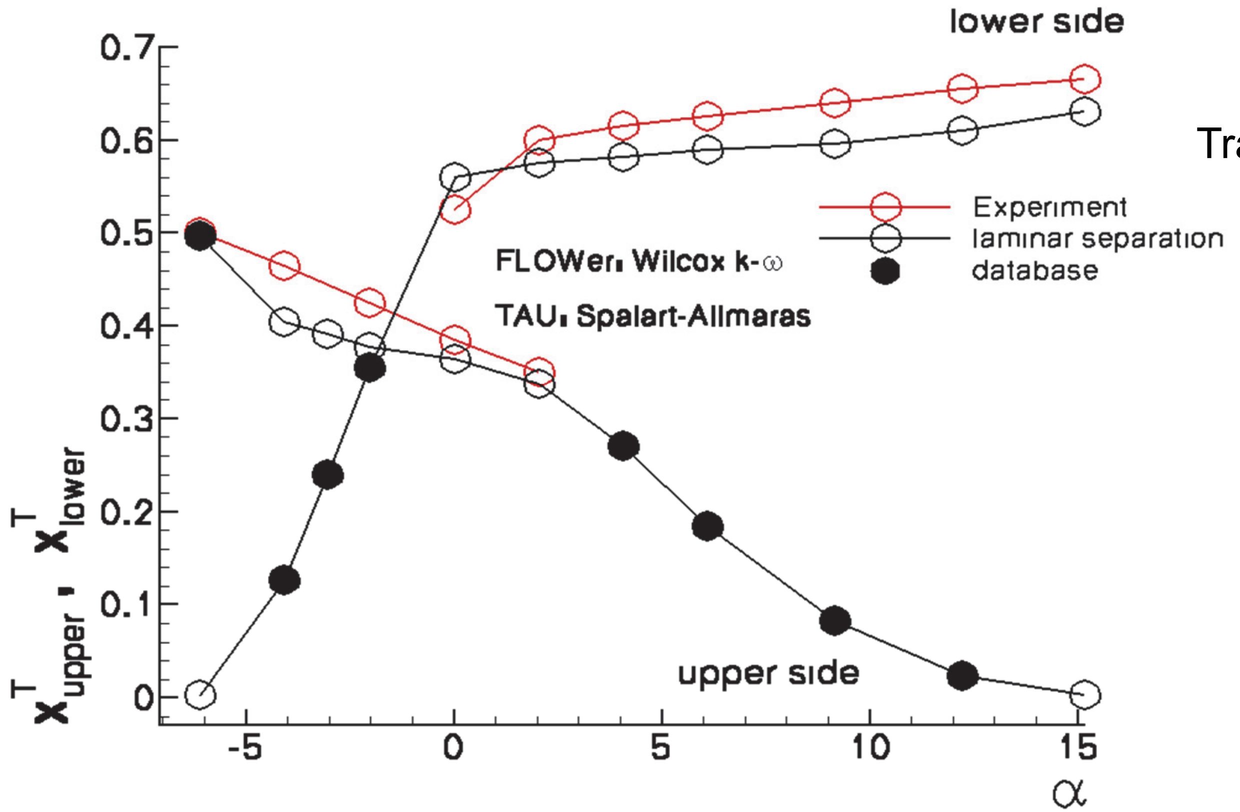

Transition locations

Transition Prediction using the e^N method
Test Cases & Results – NLF(1)-0416

- external BL approach
- BL data from BL code
- line-in-flight cuts

Natural laminar airfoil

- $M = 0.1$, $Re = 4.0x10^6$, $Tu_\infty = 0.0003 \Rightarrow N_{TScrit} = 11.0$

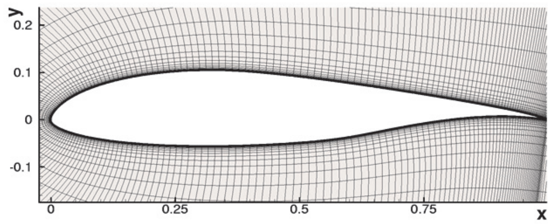

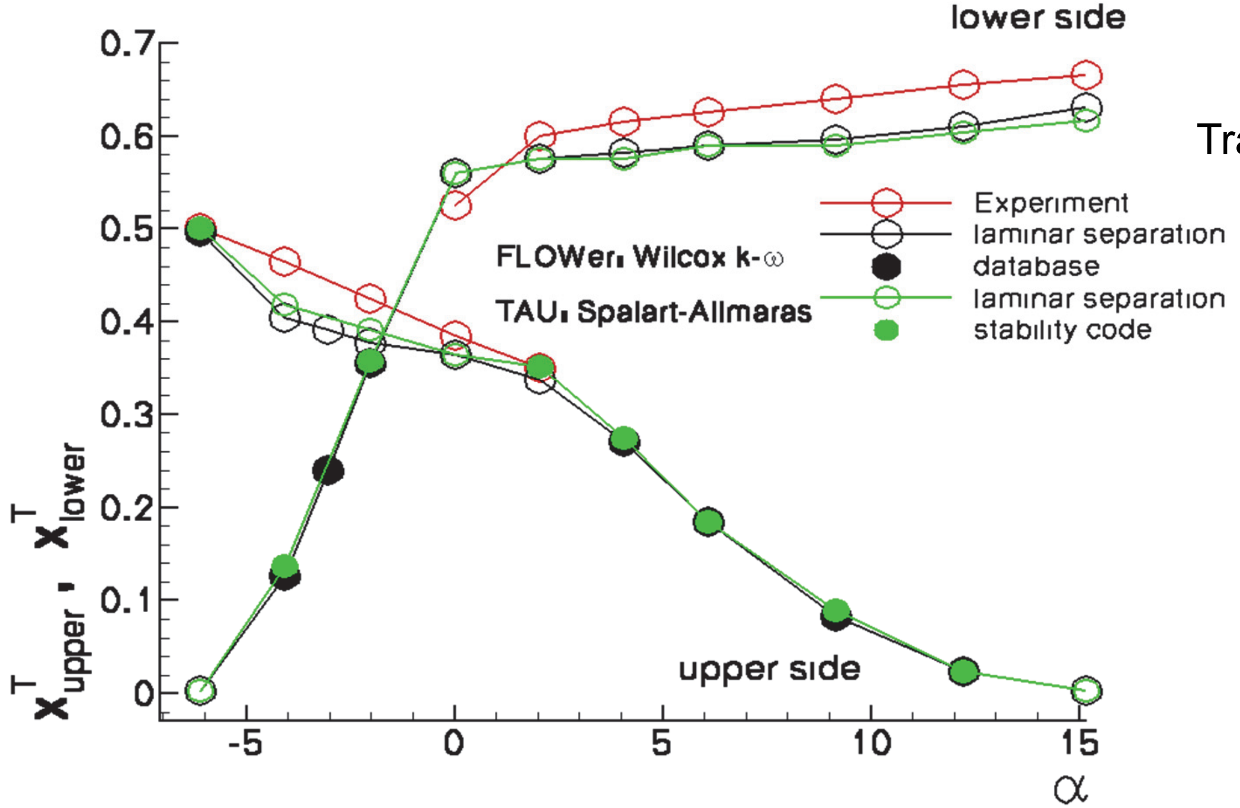

Transition locations

Transition Prediction using the e^N method
Test Cases & Results – NLF(1)-0416

- external BL approach
- BL data from BL code
- line-in-flight cuts

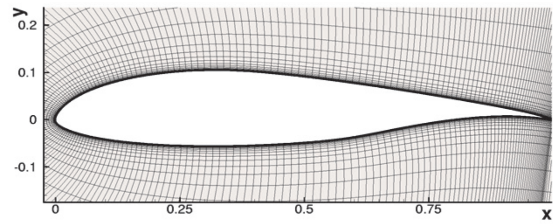

Natural laminar airfoil

- $M = 0.1$, $Re = 4.0x10^6$, $Tu_\infty = 0.0003 \Rightarrow N_{TScrit} = 11.0$

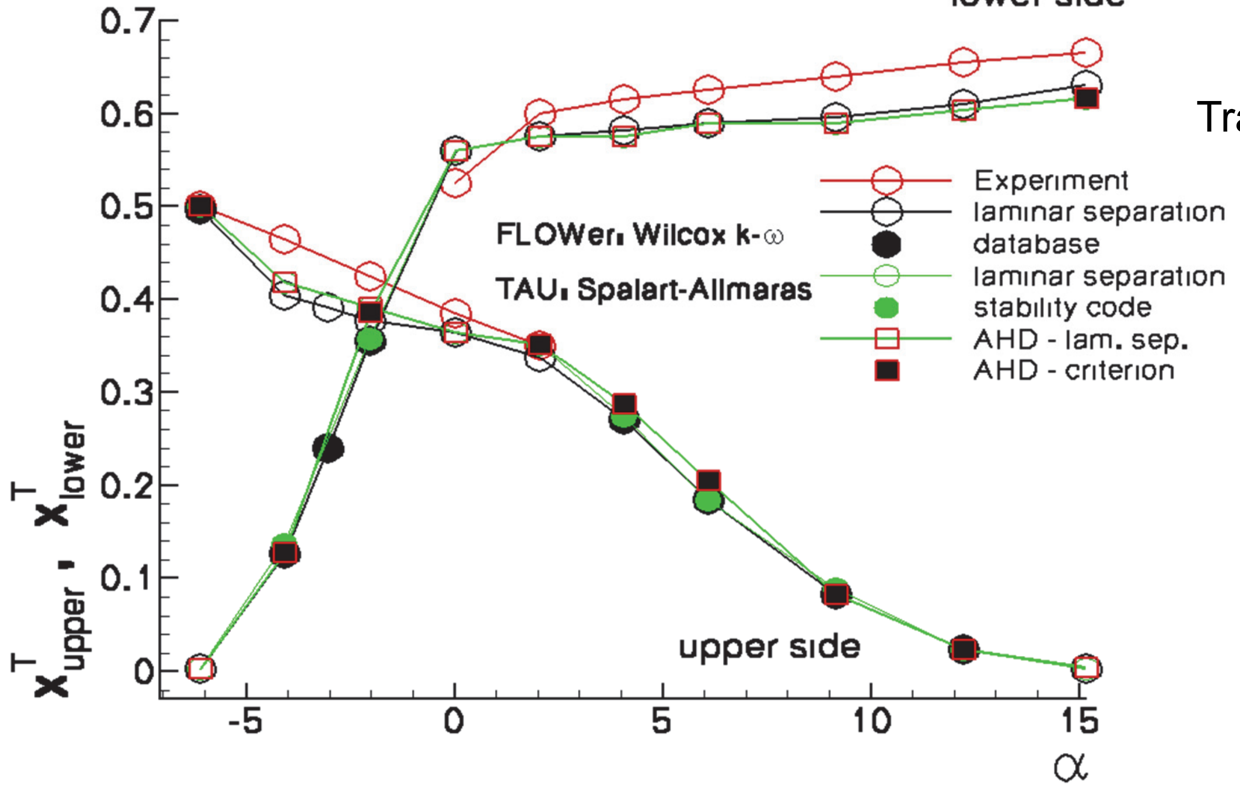

Transition locations

Transition Prediction using the e^N method
Test Cases & Results – NLR7301

- external BL approach
- BL data from BL code
- line-in-flight cuts

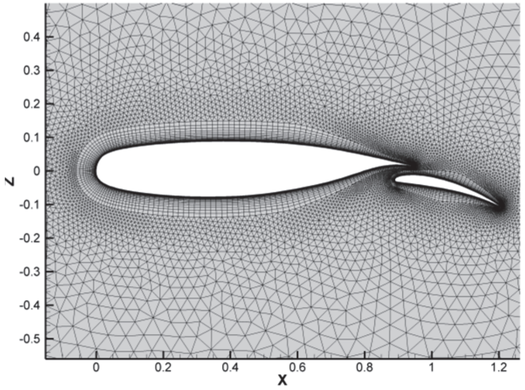

Two-element airfoil with flap

- $M = 0.185$, $Re = 1.35 \times 10^6$, $\alpha = 6.0°$
- No Tu_∞ available $\Rightarrow N_{TScrit} = 9.0$
- Calibrated by upper main transition point $\Rightarrow N_{TScrit} = 5.8$

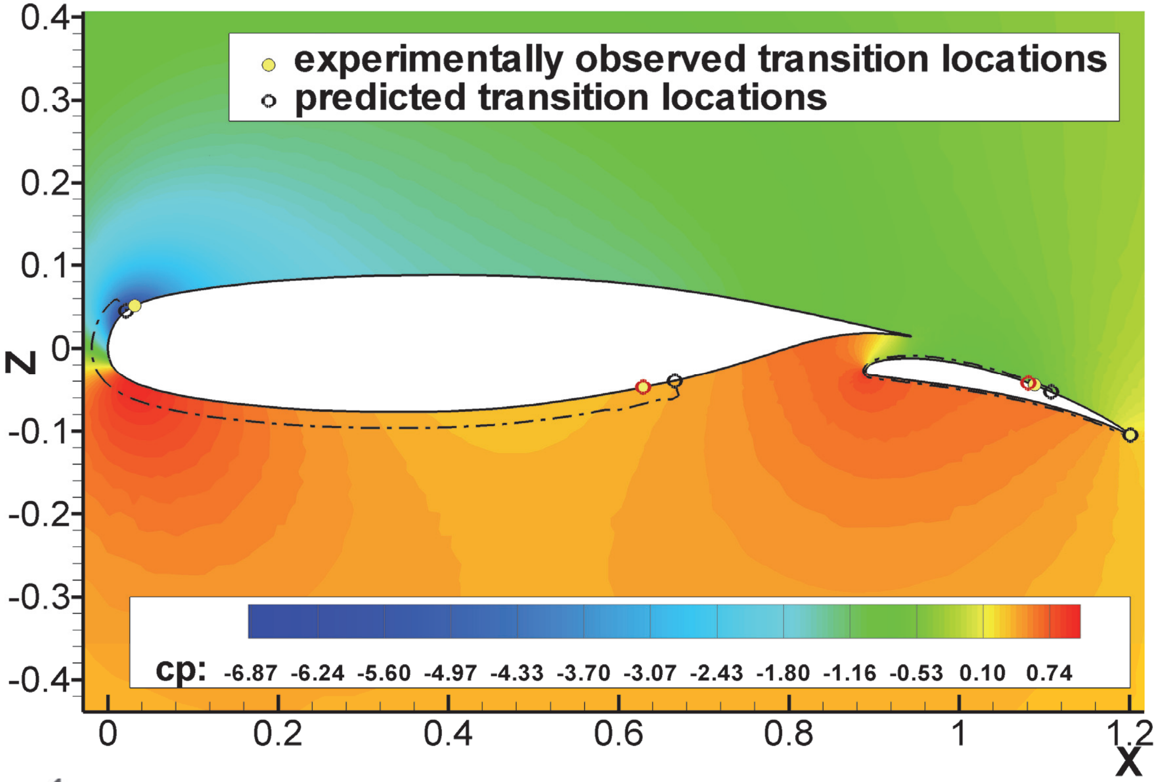

c_p-field and transition locations

Transition Prediction using the e^N method
Test Cases & Results – Swept, tapered wing

- external BL approach
- BL data from BL code
- line-in-flight cuts

Transonic laminar wing

- $M = 0.7$, $Re = 12.0x10^6$, $\alpha = 1.0°$
- $N_{TScrit} = 11.5$ (free flight)
- feasibility, no validation
- all transition locations slightly downstream of minimum pressure location due to stop of laminar BL code

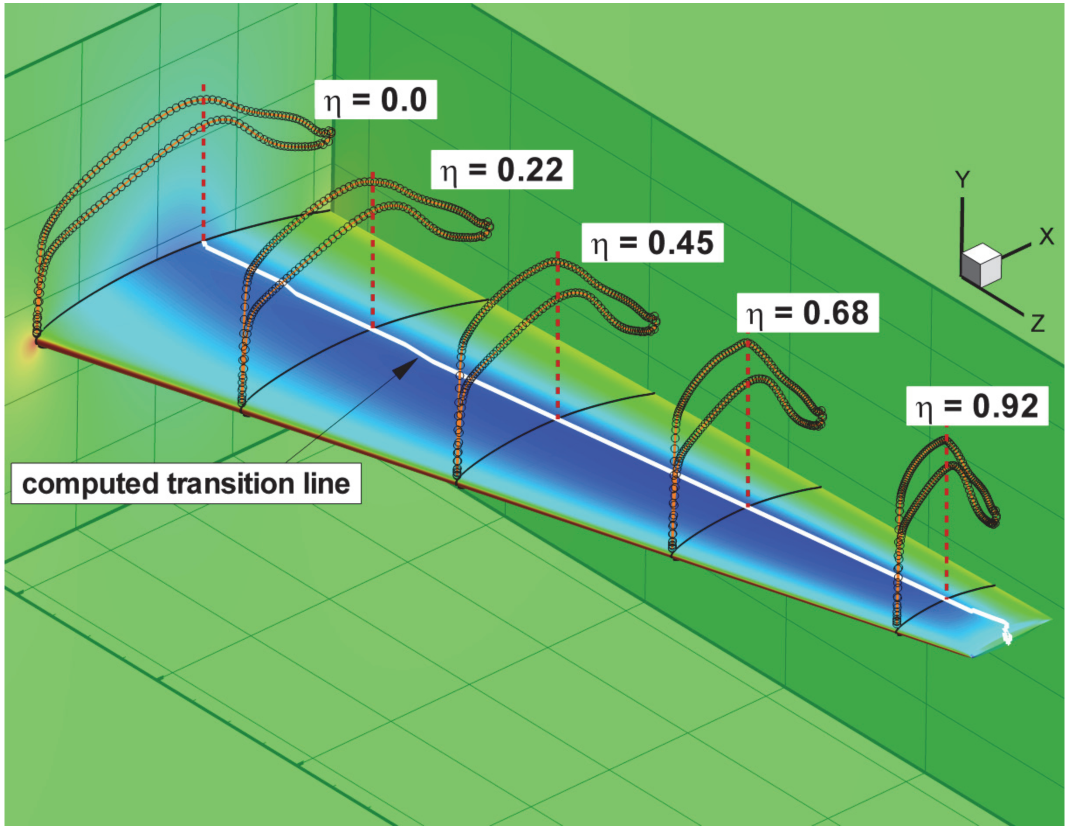

Transition Prediction using the e^N method

Test Cases & Results

ONERA M6 wing

- $M = 0.262$, $Re = 3.5 \times 10^6$

transition lines for 11 wing sections: $\eta = 0.0, 0.11, 0.22, 0.325, 0.42, 0.8, 0.86, 0.9, 0.93, 0.96, 0.975$

calibration of both N factors for lower side at $\alpha = 5°$:

$N_{CF}^{cr} = 5.157 \rightarrow \eta = 0.42$

$N_{TS}^{cr} = 4.75 \rightarrow \eta = 0.93$

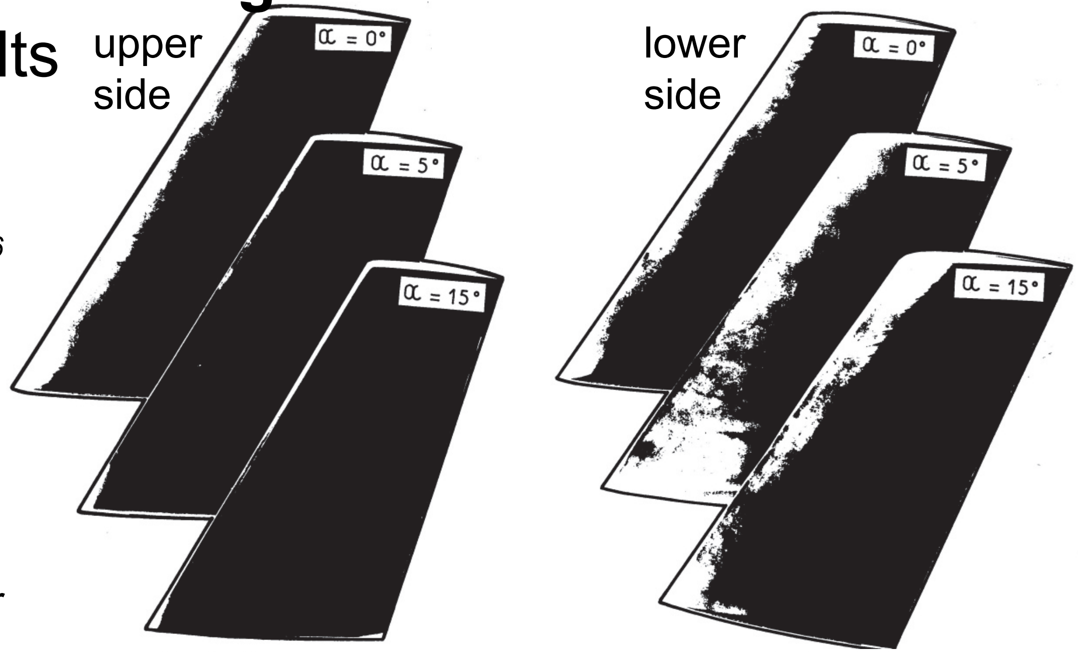

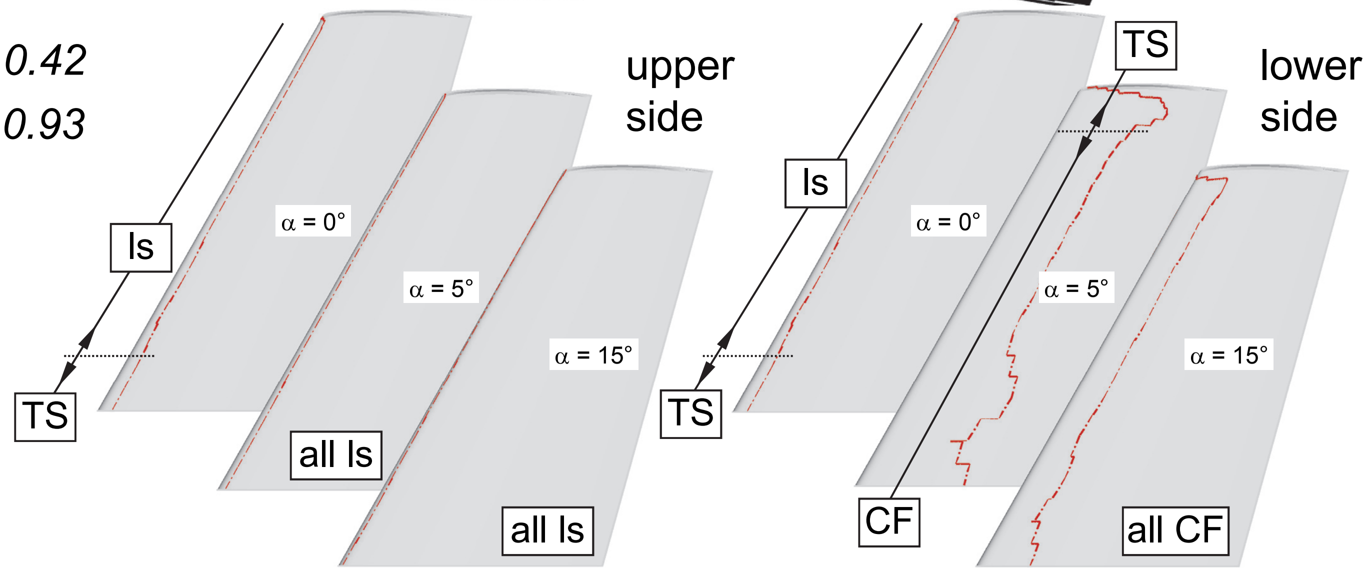

- external BL approach
- BL data from BL code
- line-in-flight cuts

Transition Prediction using the e^N method
Test Cases & Results – DLR F11 (KH3Y)

- external BL approach
- BL data from BL code
- line-in-flight cuts

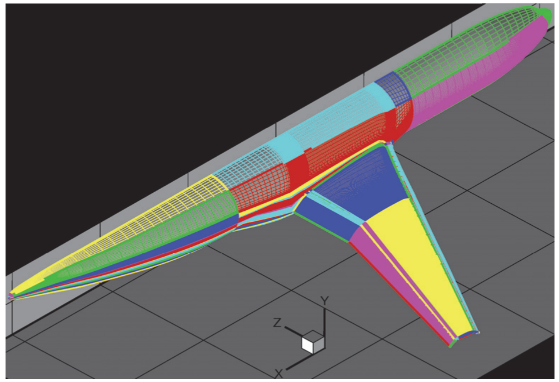

block-structured computation

Wing-Body High-Lift Configuration

- *$M = 0.174$, $Re = 1.35x10^6$, $\alpha = 10.0°, 14.0°$*
- *$N_{TScrit} = 4.9$, calibration for $\alpha = 10°$ hot film on main wing upper side at 68% span $\rightarrow (x^T/c)^{main} = 0.08$*
- *no indications for CF $\Rightarrow N_{CFcrit} = N_{TScrit}$*

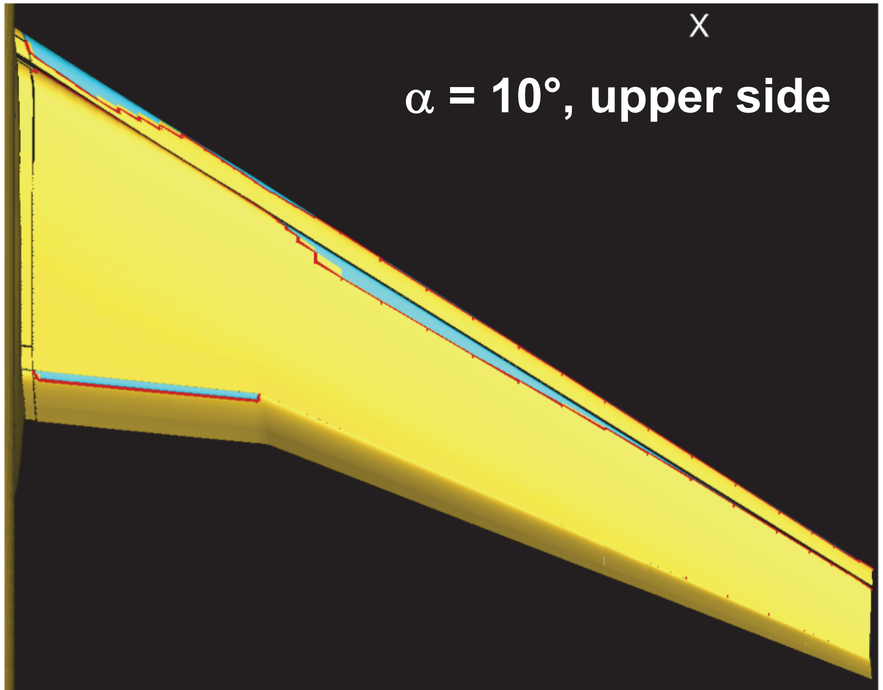

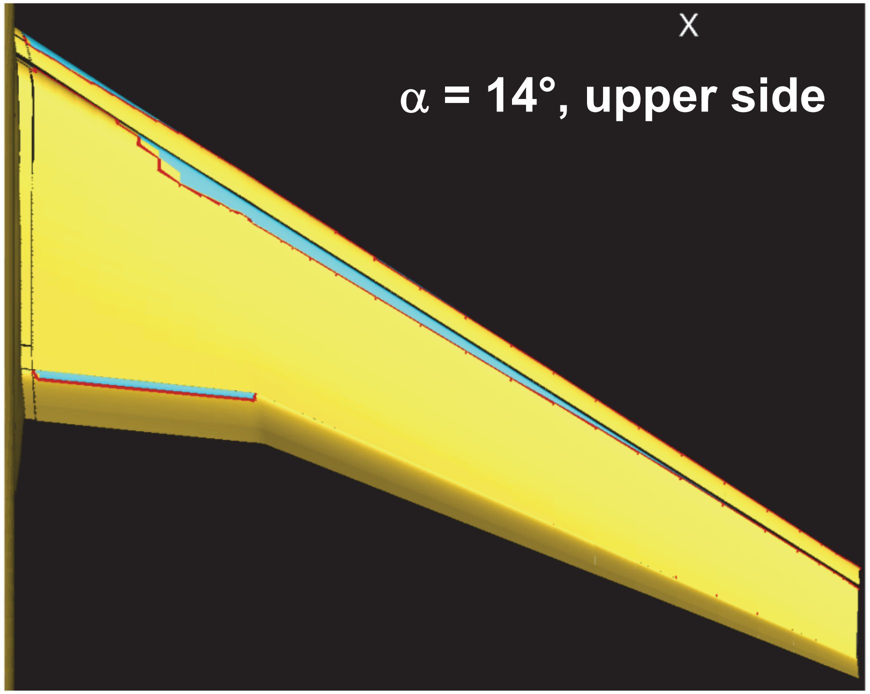

Transition Prediction using the e^N method
Test Cases & Results – DLR F11 (KH3Y)

- external BL approach
- BL data from BL code
- line-in-flight cuts

c_p-distributions

$\alpha = 14.0°$

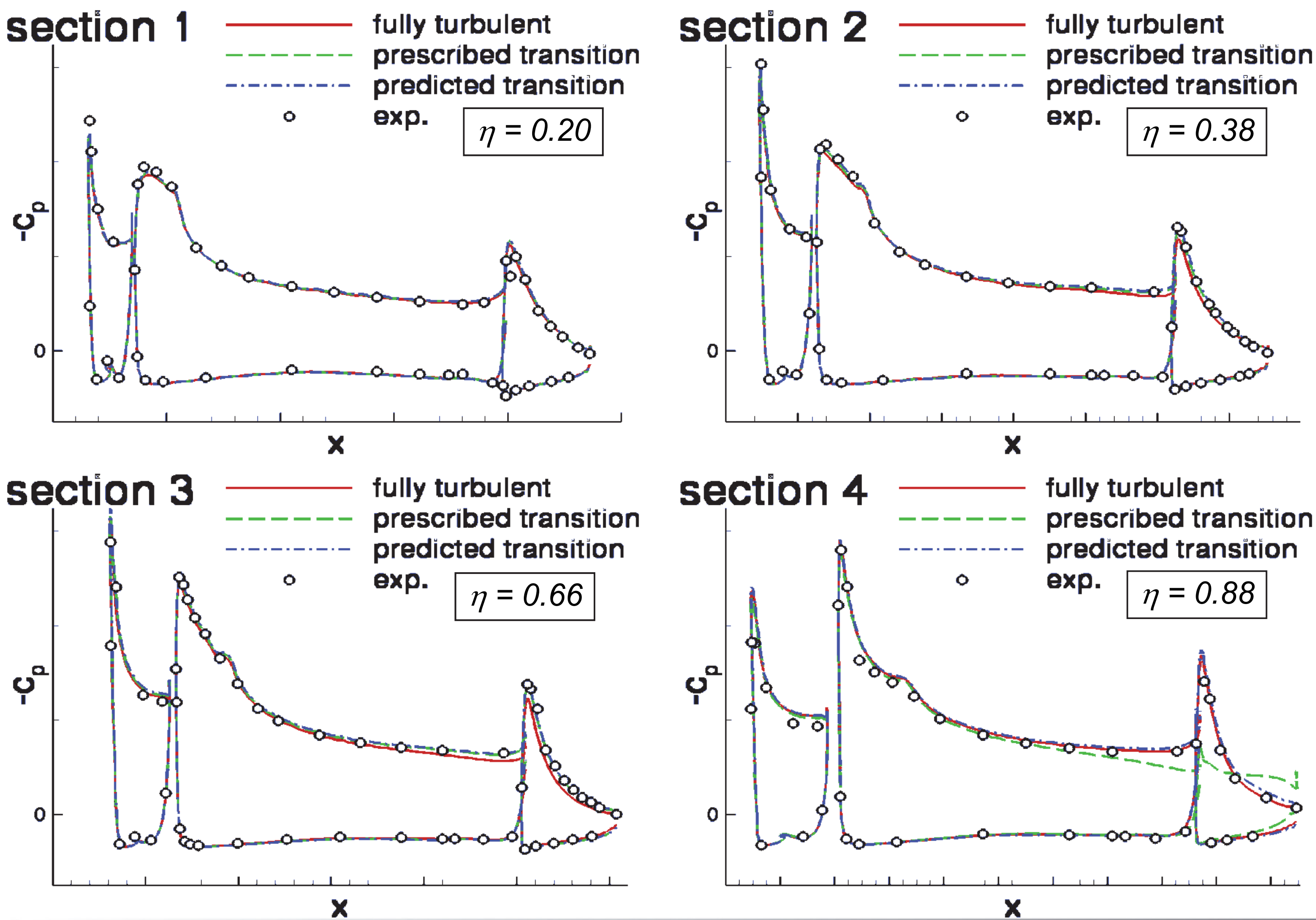

Transition Prediction using the e^N method
Test Cases & Results – DLR F11 (KH3Y)

- external BL approach
- BL data from BL code
- line-in-flight cuts

Wing-Body High-Lift Configuration

➢ $M = 0.174$, $Re = 1.35x10^6$, $\alpha = 10.0°, 14.0°$

Structured vs. unstructured results

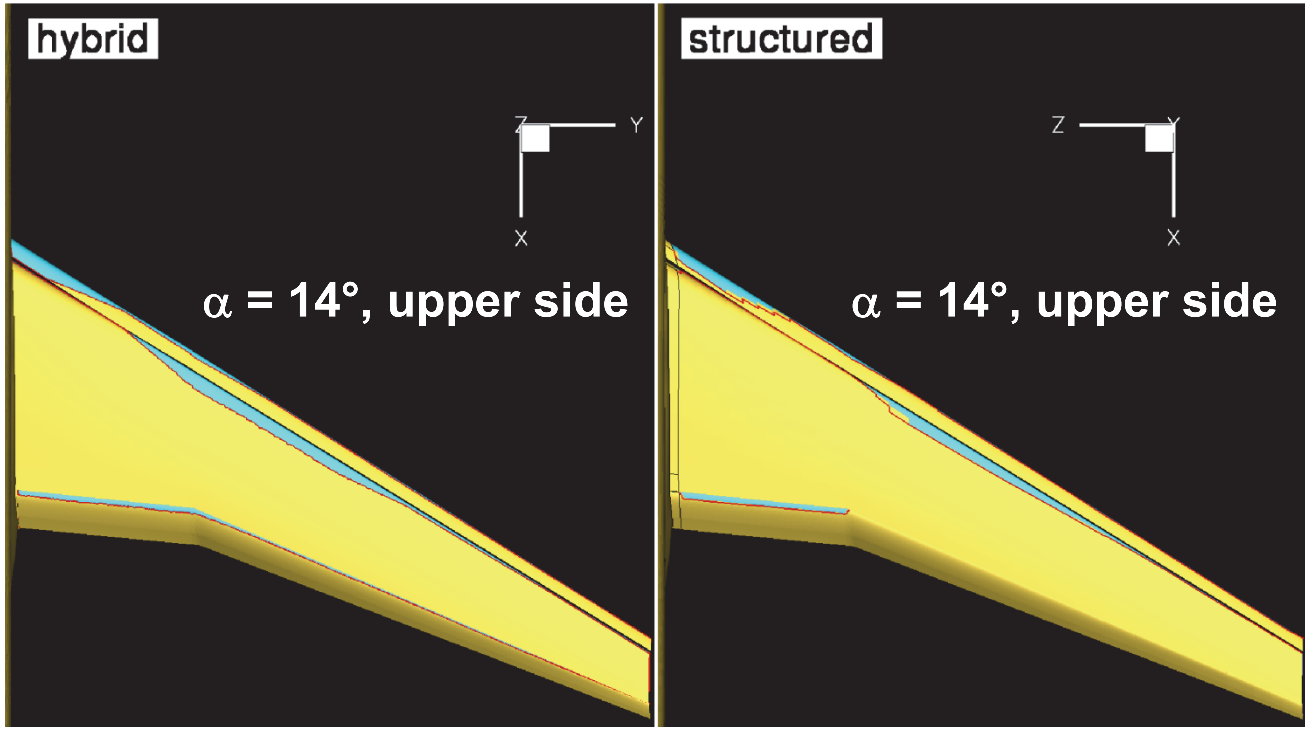

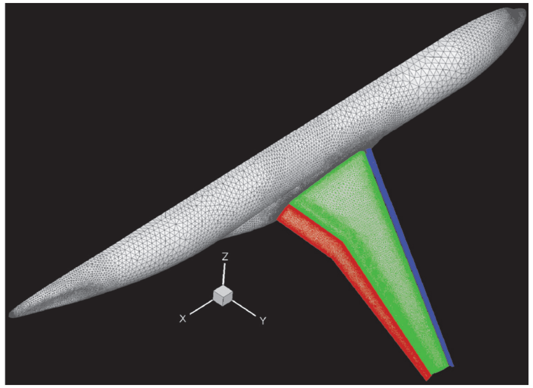

hybrid-unstructured computation

Experiment vs. computation

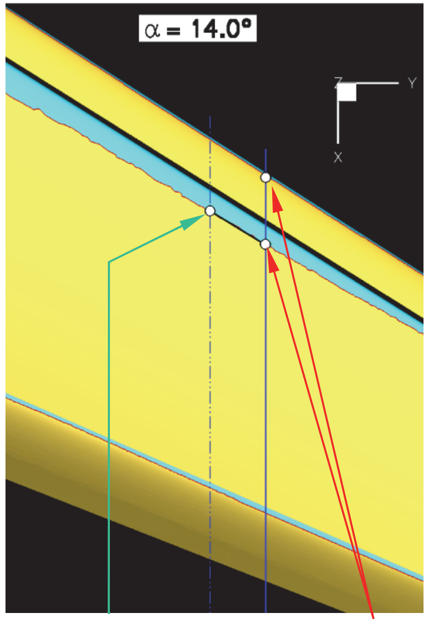

calibration point for N_{TS}

experimental transition locations

Transition Prediction using the e^N method

Test Cases & Results – 6:1 prolate spheroid

- internal BL approach
- BL data from RANS
- inviscid streamlines

Simplified fuseláge

- *M = 0.03*
- *Re = **1.5x10^6***
- α = ***10°***

- Determined by numerical investigation
- modeling of the interaction of TS and CF waves
- $N_{TS,crit}$ = 8.0, $N_{CF,crit}$ = 5.5

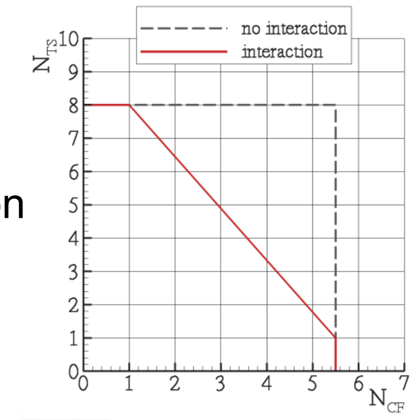

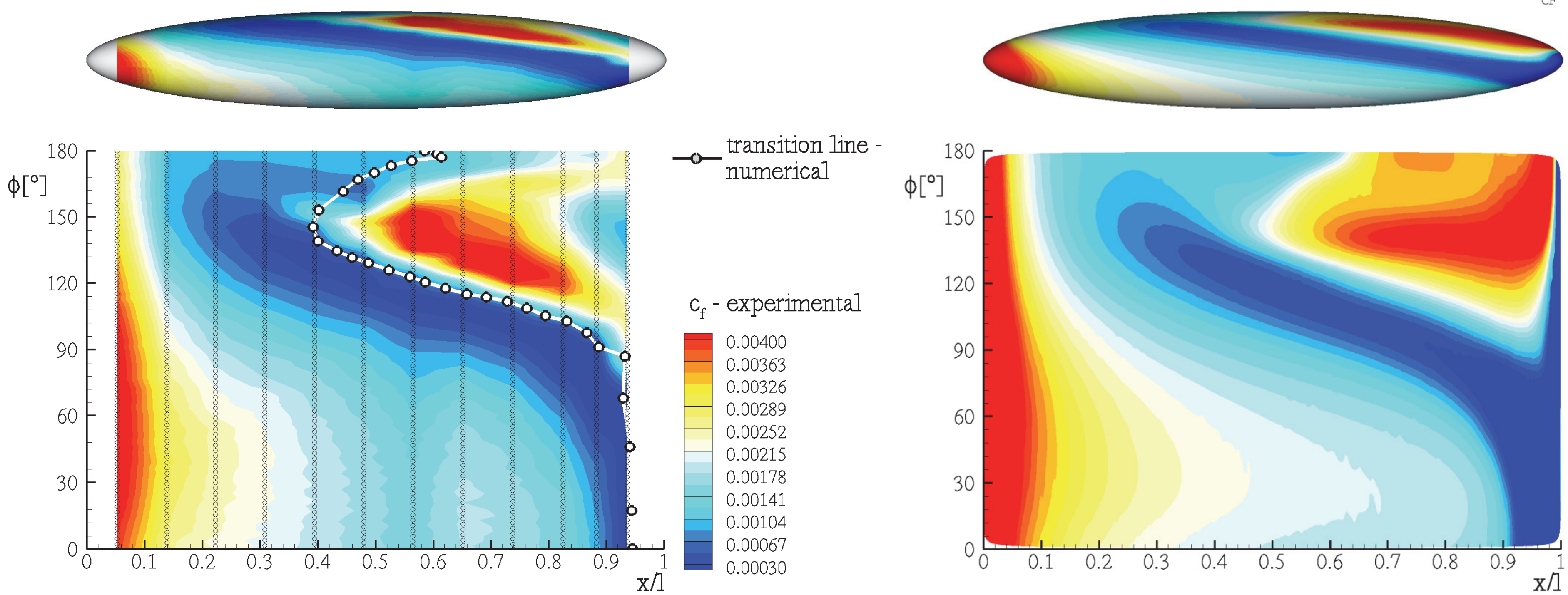

TS dominated transition (no interaction of modes)

Transition Prediction using the e^N method

Test Cases & Results – 6:1 prolate spheroid

- internal BL approach
- BL data from RANS
- inviscid streamlines

Simplified fuselage

- *M = 0.13*
- *Re = **6.5x10⁶***
- α = ***10°***

- Determined by numerical investigation
- modeling of the interaction of TS and CF waves
- $N_{TS,crit} = 8.0$, $N_{CF,crit} = 5.5$

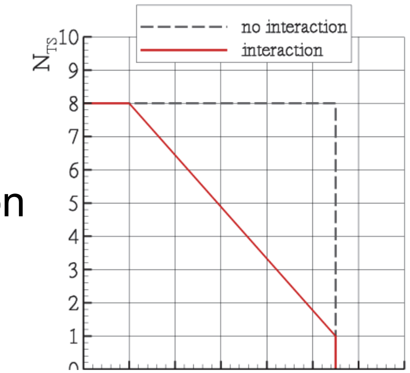

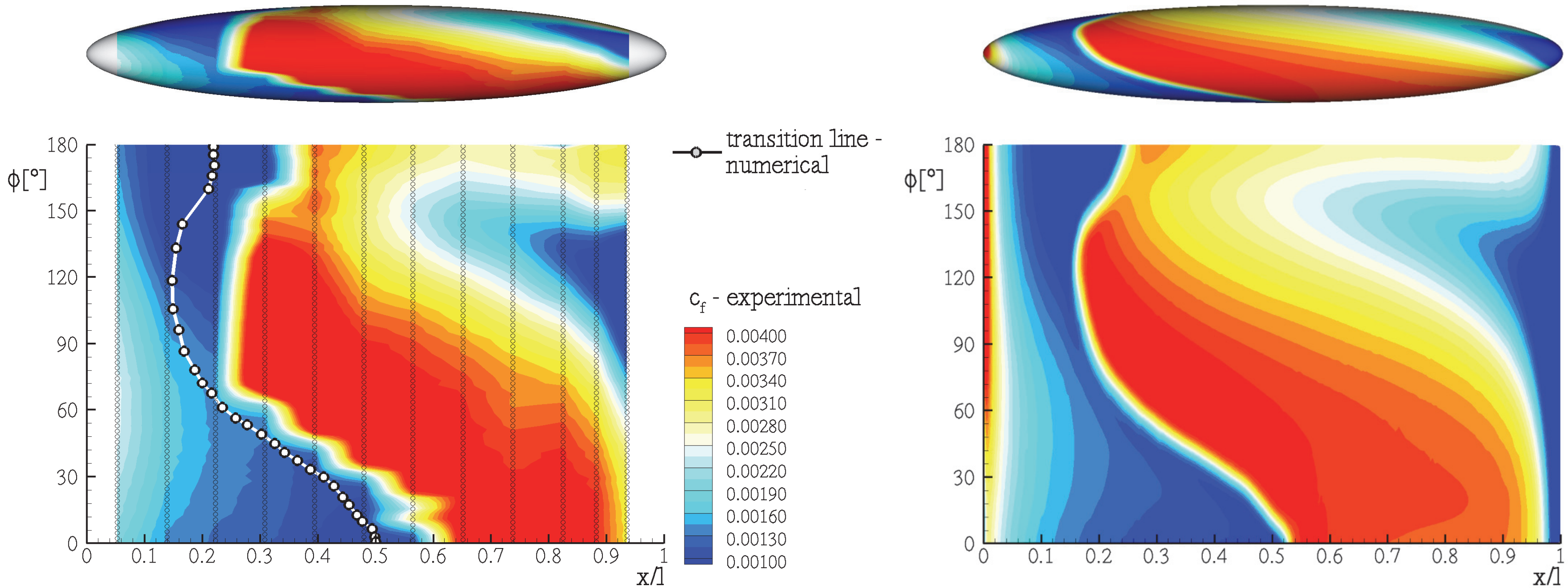

TS and CF transition (strong interaction of modes)

Transition Prediction using the e^N method
Test Cases & Results – 6:1 prolate spheroid

- internal BL approach
- BL data from RANS
- inviscid streamlines

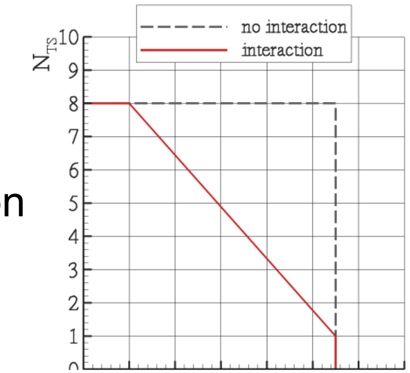

Simplified fuselage
- $M = 0.13$
- $Re = \mathbf{6.5x10^6}$
- $\alpha = \mathbf{15°}$

- Determined by numerical investigation
- modeling of the interaction of TS and CF waves
- $N_{TS,crit} = 8.0$, $N_{CF,crit} = 5.5$

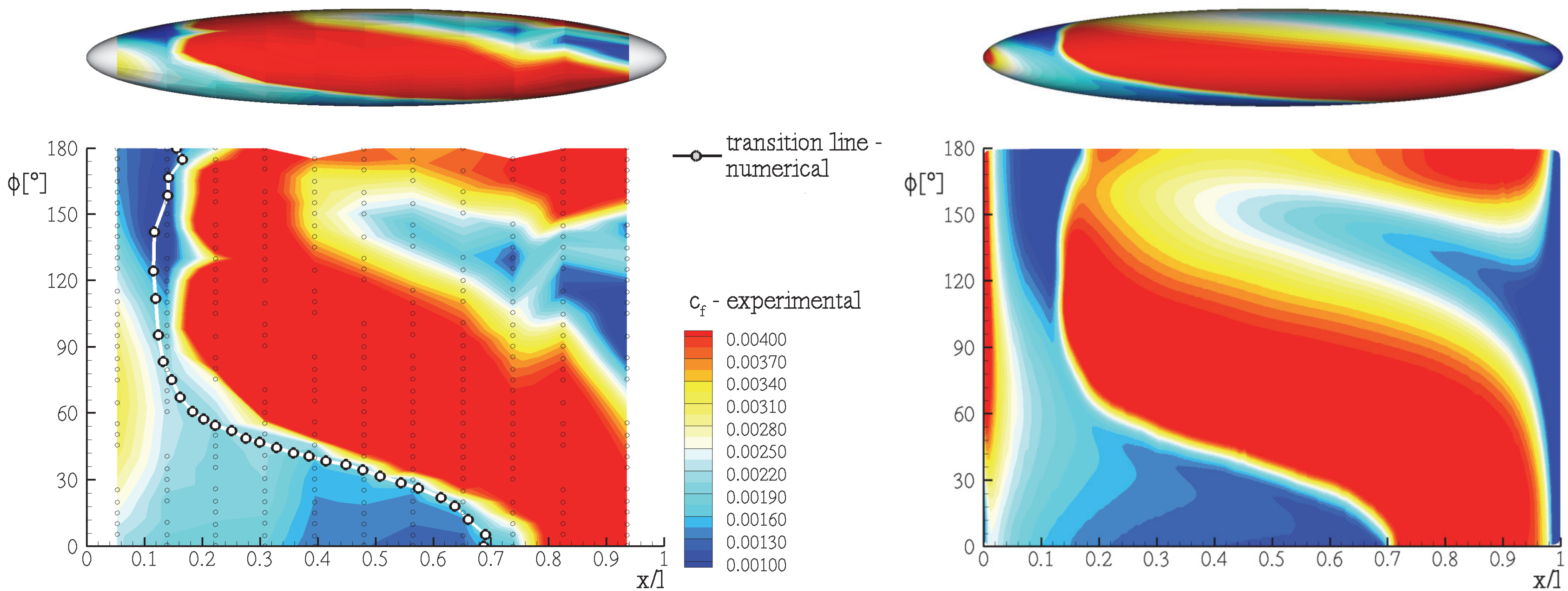

CF dominated transition (slight interaction of modes)

Transition Prediction using the e^N method

Test Cases & Results – Some more examples

Full transport aircraft

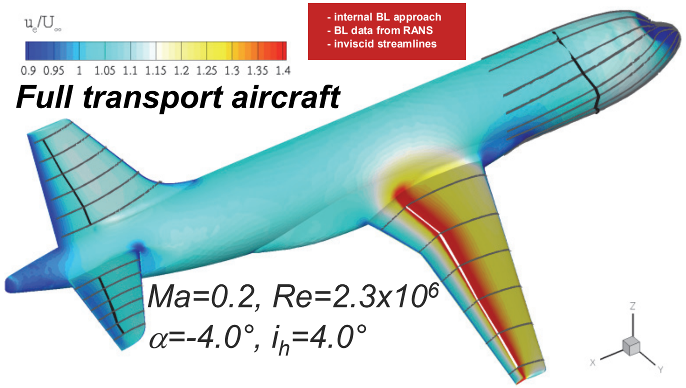

$Ma=0.2$, $Re=2.3 \times 10^6$
$\alpha=-4.0°$, $i_h=4.0°$

Wing with winglet

$U_\infty = 50$ m/s
$Re = 1.3 \times 10^6$

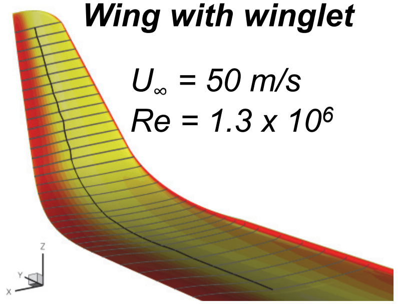

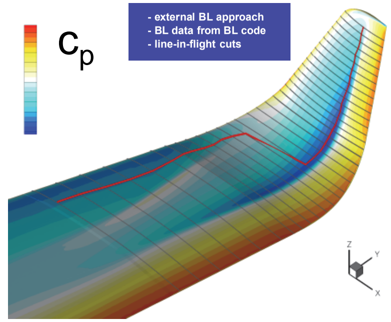

Nacelle of aircraft enigne

- internal BL approach
- BL data from RANS
- inviscid streamlines

$Re = 3.0 \times 10^6$
$Ma = 0.78$
$\alpha = 1.3°$

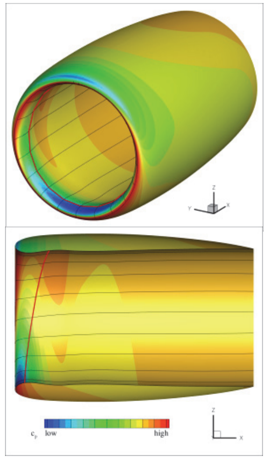

Technische Universität Braunschweig

Wing-Body with 4-element wing

- 388 cuts overall
- 536 transition predictions per step
- 96 processes

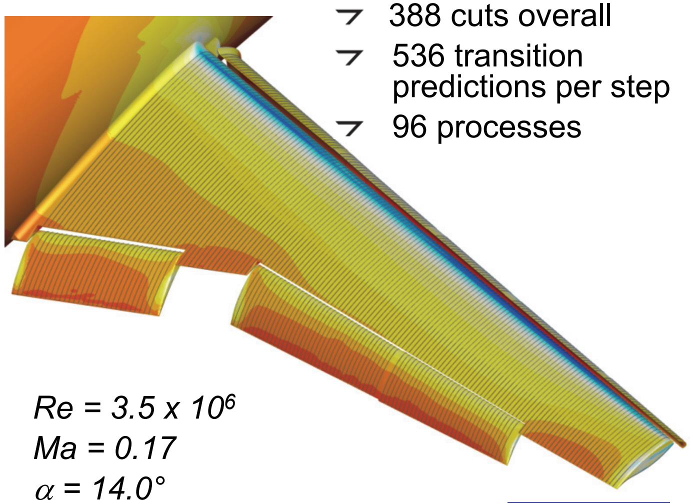

$Re = 3.5 \times 10^6$
$Ma = 0.17$
$\alpha = 14.0°$

- external BL approach
- BL data from BL code
- line-in-flight cuts

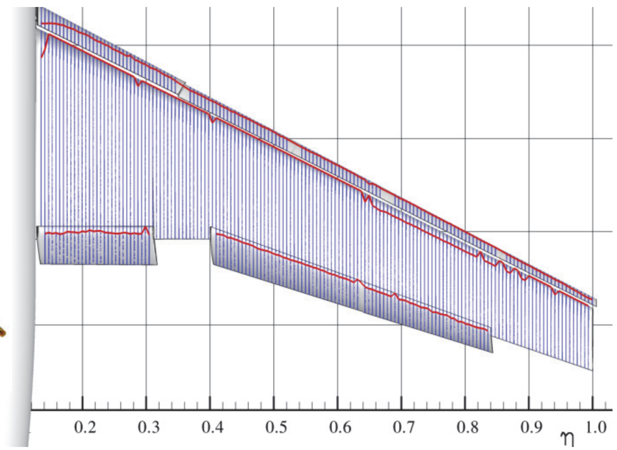

Helicopter fuselage

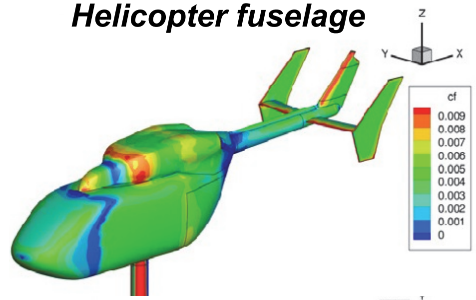

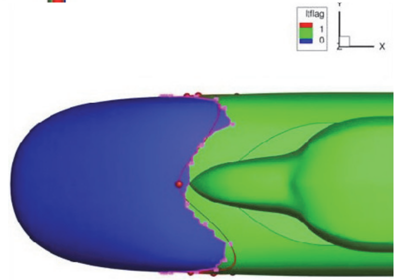

- internal BL approach
- BL data from RANS
- inviscid streamlines

The γ-$Re_{\theta,t}$ Transport Equation Model
Test Original Model

Basics of correlation based transition modeling approach

- Two transport equations with structure similar to turbulence model equation

- A key quantity is the following Reynolds number correlation

$$\frac{Re_{\nu,\max}}{Re_{\theta t}} = 2.193$$

- Correlation of local to non-local quantities

$$\mathrm{Re}_{\nu,\max} = f\left(\mathrm{y}, \nu, \frac{\mathrm{du}}{\mathrm{dy}}\right) \longrightarrow$$ **Locally** available in a RANS-based CFD Code

$$\mathrm{Re}_{\theta\mathrm{t}} = f\left(\theta, \nu, \mathrm{u}\right) \longrightarrow$$ **Non-local** quantity, θ contains information about transition location

- Approach given by Liepmann (1943) and later by van Driest/Blumer (1963):

  „If the ratio of turbulent stress to viscous stress will reach a certain value in the boundary layer, transition will take place.“

The γ-$Re_{\theta,t}$ Transport Equation Model
Test Original Model

Basics of correlation based transition modeling approach

$$\frac{\tau_{\mathrm{turb}}}{\tau_{\mathrm{visc}}} = \frac{\rho \overline{\mathrm{u}'\mathrm{u}'}}{\mu \frac{\mathrm{du}}{\mathrm{dy}}} = \frac{\rho \mathrm{y}^2 \left(\frac{\mathrm{du}}{\mathrm{dy}}\right)^2}{\mu \frac{\mathrm{du}}{\mathrm{dy}}} = \underbrace{\frac{\mathrm{y}^2}{\nu} \frac{\mathrm{du}}{\mathrm{dy}}}_{Re_{\nu,\mathrm{x}}}$$

Uses mixing length approach and the wall distance y as the characteristic mixing length.

- Stress ratio at transition onset $\longrightarrow$ $\overbrace{\left.\frac{\mathrm{y}^2}{\nu} \frac{\mathrm{du}}{\mathrm{dy}}\right|_{\mathrm{trans}}}^{Re_{\nu,\mathrm{x,trans}}} = \mathrm{const.}$

- Usage of Pohlhausen approximation for boundary layer velocity u, some transformations and the choice of a suitable transition criterion, e.g.

$$Re^{\star}_{\theta\mathrm{t}} = f\left(\mathrm{Tu}, \lambda\right)$$

lead to

$$\frac{Re_{\nu,\mathrm{x,max}}}{Re_{\theta\mathrm{t}}} = 2.193$$

The γ-$Re_{\theta,t}$ Transport Equation Model
Test Original Model

- **Intermittency** transport equation (fraction of time the flow is turbulent compared to a total time, $\gamma = 0$: laminar flow, $\gamma = 1$: turbulent flow)

$$\frac{\partial(\rho\gamma)}{\partial \mathrm{t}} + \frac{\partial(\rho \mathrm{u_i}\gamma)}{\partial \mathrm{x_j}} = \mathrm{P}_\gamma + \mathrm{D}_\gamma + \frac{\partial}{\partial \mathrm{x_j}}\left[\left(\mu + \frac{\mu_\mathrm{t}}{\sigma_\gamma}\right)\frac{\partial\gamma}{\partial \mathrm{x_j}}\right]$$

- Production $\mathrm{P}_\gamma = f\left(\mathbf{F_{onset}}, \mathbf{F_{length}}, \gamma, \rho, S, \mathrm{c_i}\right)$
- Destruction $\mathrm{D}_\gamma = f\left(\mathbf{F_{turb}}, \gamma, \rho, \Omega, \mathrm{c_i}\right)$

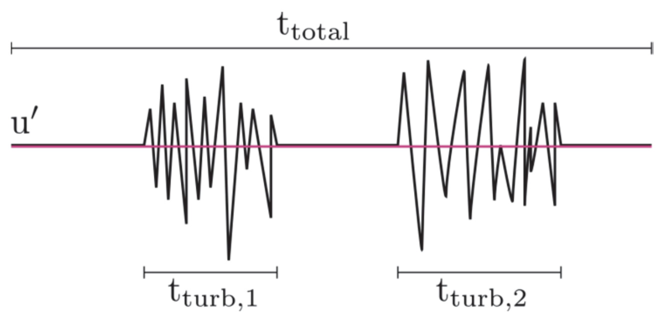

$\mathbf{F_{onset}} = f\left(Re_\nu / Re_{\theta c} / 2.193, \mu_\mathrm{t}/\mu\right)$ triggers γ production

$\mathbf{F_{length}} = f\left(\tilde{R}e_{\theta \mathrm{t}}\right)$ defines length of transition region

$\mathbf{F_{turb}} = f\left(\mu_\mathrm{t}/\mu\right)$ destroys γ values where μ_t/μ is very low

The γ-$Re_{\theta,t}$ Transport Equation Model
Test Original Model

- Transport equation for the **Reynolds number based on momentum thickness at transition onset**

$$\frac{\partial\left(\rho\tilde{Re}_{\theta t}\right)}{\partial t}+\frac{\partial\left(\rho u_i\tilde{Re}_{\theta t}\right)}{\partial x_j}=P_\theta+\frac{\partial}{\partial x_j}\left[\sigma_\theta\left(\mu+\mu_t\right)\frac{\partial\tilde{Re}_{\theta t}}{\partial x_j}\right]$$

- Production/Destruction $\quad P_\theta=f\left(\mathbf{Re}^\star_{\theta t},\tilde{Re}_{\theta t},\mathbf{F}_\theta,c_i\right)$

$\mathbf{F}_\theta$: boundary-layer detector switches on/off P_θ inside/outside BL

$\mathbf{Re}^\star_{\theta t}=f\left(Tu,\lambda\right)$: empirical transition criterion

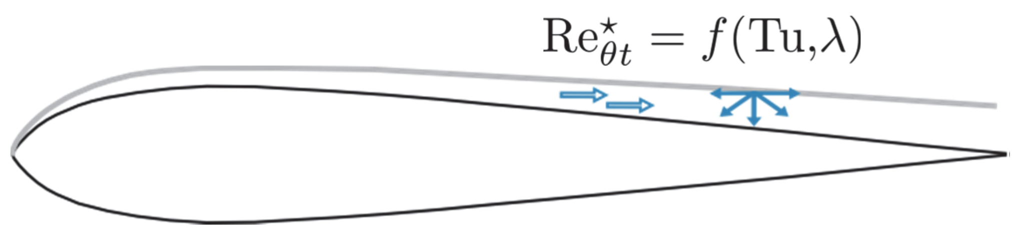

The γ-$Re_{\theta,t}$ Transport Equation Model
Test Original Model

- The intermittency is coupled to the production and destruction terms of the k-equation of the Menter SST k-ω turbulence model

$$\mathrm{P}_\mathrm{k}^\star = \gamma_\mathrm{eff}\mathrm{P}_\mathrm{k}$$

$$\mathrm{D}_\mathrm{k}^\star = \min(\max(\gamma_\mathrm{eff}, 0.1), 1.0)\mathrm{D}_\mathrm{k}$$

$$\gamma_\mathrm{eff} = \max[\gamma, \gamma_\mathrm{sep}]$$

- From a technical point of view, the model is suitable for any type of RANS solver and for arbitary 3D geometrical configurations and any kind of flow.
- It covers streamwise transition mechanisms, such as Tollmien-Schlichting-like transition, by-pass transition and separation induces transition.
- It does not cover cross flow (CF) transition, typical for 3D flows.

The γ-$Re_{\theta,t}$ Transport Equation Model
Test Cases & Results – AS-A & NLF(1)-0416

- The γ-$Re_{\theta t}$ model was implemented into the DLR TAU code and validated on various two-dimensional test cases like the AS-A airfoil and the NLF(1)-0416 airfoil.

- AS-A airfoil

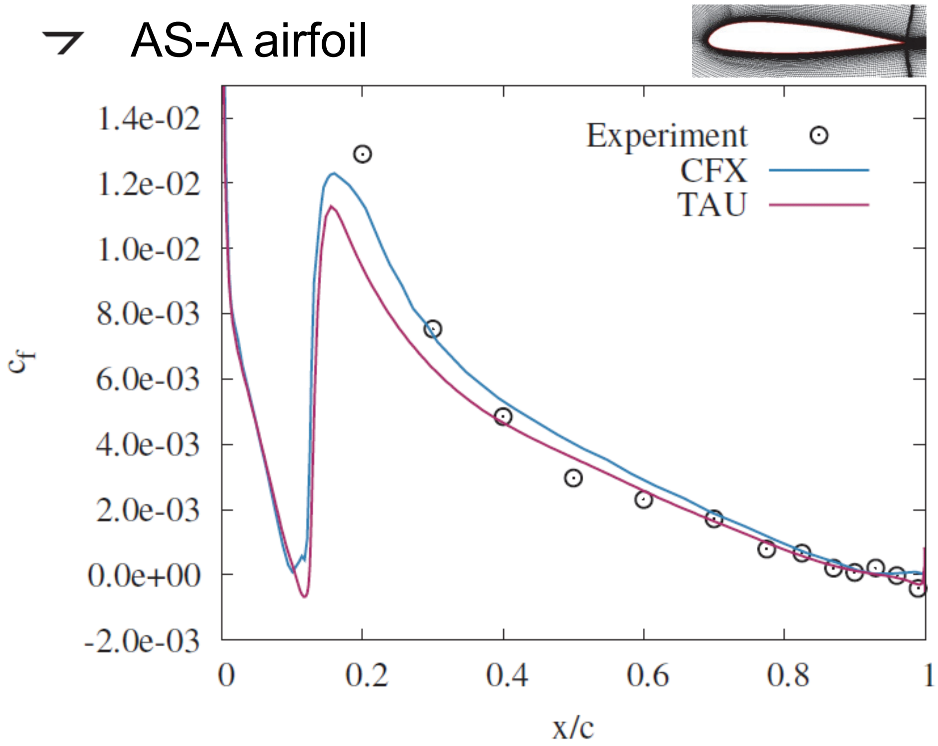

- NLF(1)-0416 airfoil

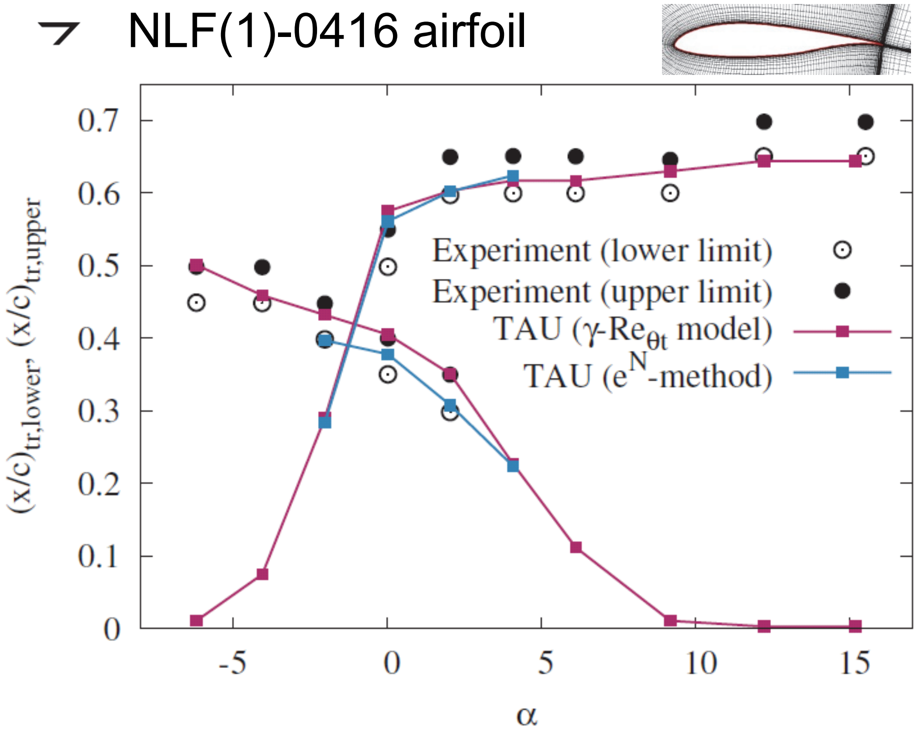

The γ-$Re_{\theta,t}$ Transport Equation Model
Test Cases & Results – 6:1 prolate spheroid

- c_f-distribution for $Re = 1.5 \times 10^6$, $M = 0.03$, $\alpha = 5°$ pure TS transition

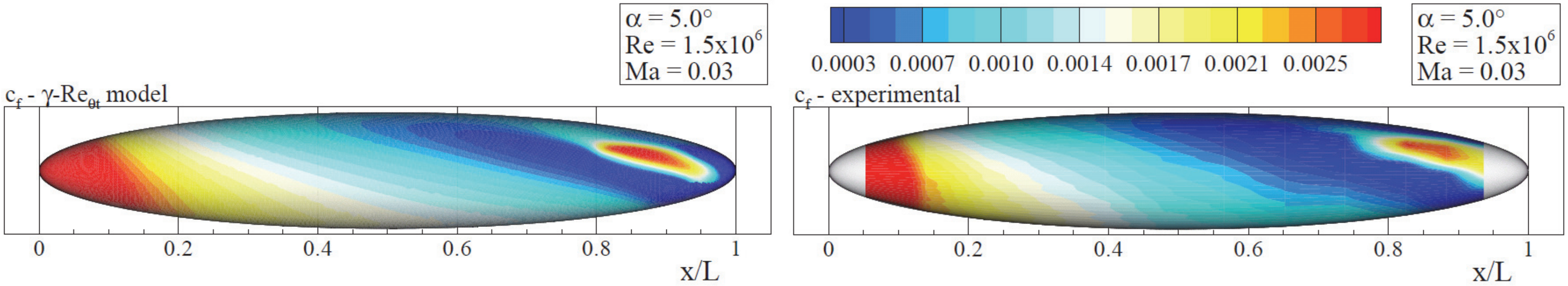

- c_f-distribution for $Re = 1.5 \times 10^6$, $M = 0.03$, $\alpha = 10°$ pure TS transition

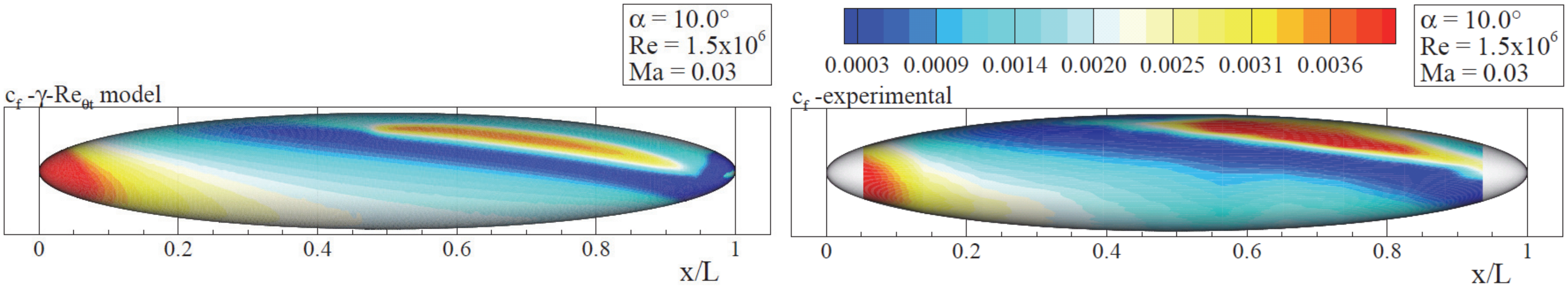

The γ-$Re_{\theta,t}$ Transport Equation Model
Test Cases & Results – 6:1 prolate spheroid

- c_f-distribution for Re = 6.5×10^6 , M = 0.13, α = 5°

TS + CF transition

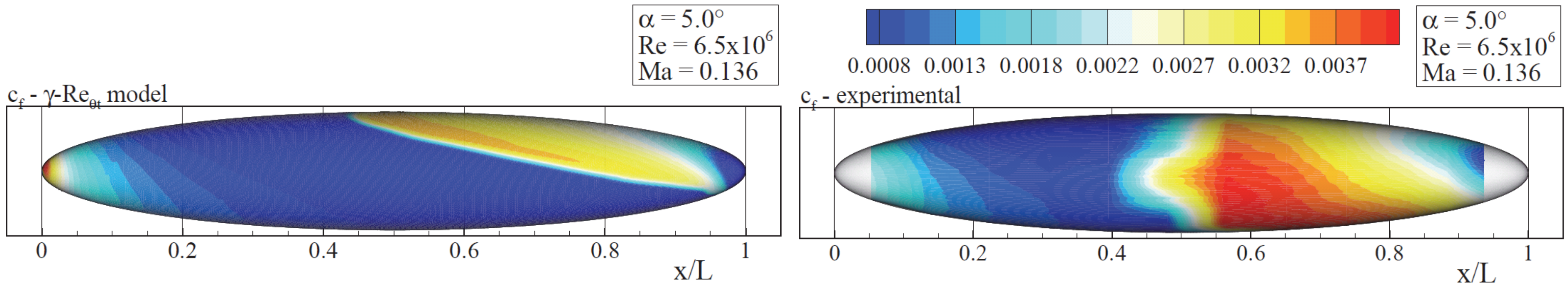

- c_f-distribution for = 6.5×10^6 , M = 0.136, α = 15°

pure CF transition

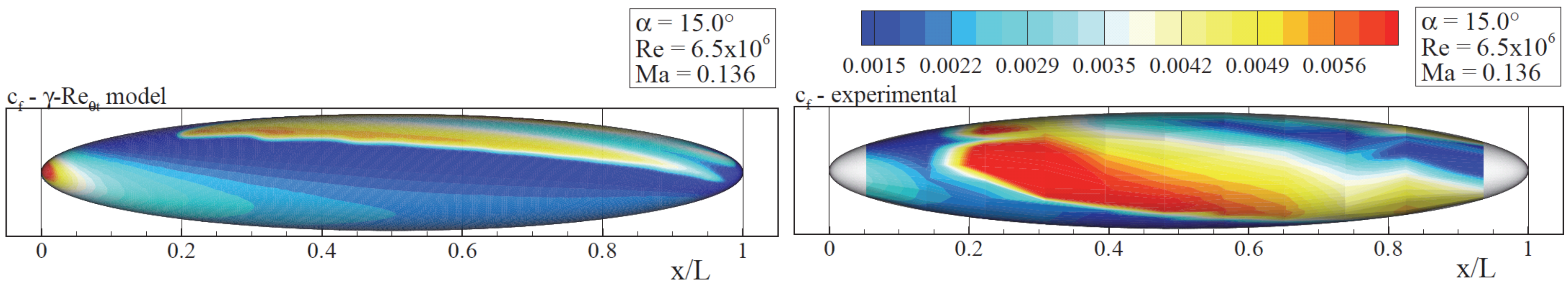

The γ-$Re_{\theta,t}$ Transport Equation Model
Extension to Three-dimensional Flows

- The approach of the original model was tranferred to the spanwise flow direction $\longrightarrow$ γ-$Re_{\theta,t}$-$Re_{\delta 2,t}$
- As no analytical approximation exists for the velocity profile in crossflow direction the **Falkner-Skan-Cooke (FSC) similarity solution** was used to approximate the velocity profiles in three-dimensional boundary layers.
- C_1 transition criterion for CF transition: $Re_{\delta 2} = Re_{\delta 2}(\mathrm{H}),\ \mathrm{H} = \delta 1/\Theta$
- The same formalism as for the original model leads to:

$\delta 1$: displacement thickness of streamwise velocity profile

Θ: momentum loss thickness of streamwise velocity profile

$\delta 2$: displacement thickness of cross flow velocity profile

$$\frac{\mathrm{Re}_{\nu,\mathrm{z,max}}}{\mathrm{Re}_{\delta 2}} = f\left(\vartheta, \mathrm{FSC} - \mathrm{eq.}(\beta_h)\right)$$

Local sweep angle of stream line

Here, two ordinary coupled differential equations – the FSC equations – are solved numerically at each grid point.

Hartree parameter of the FSC equations contains the streamwise pressure gradient

The γ-$Re_{\theta,t}$ Transport Equation Model
Extension to Three-dimensional Flows

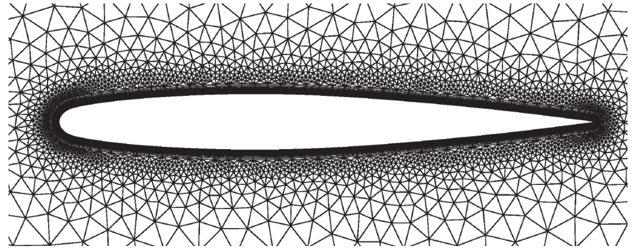

ONERA D – infinite swept wing (2.5D)

- *Low M, Re = 1.0 x 10^6 & 1.5 x 10^6, α = -6°, 40° < Φ_∞ < 60°*
- *Pure CF transition*

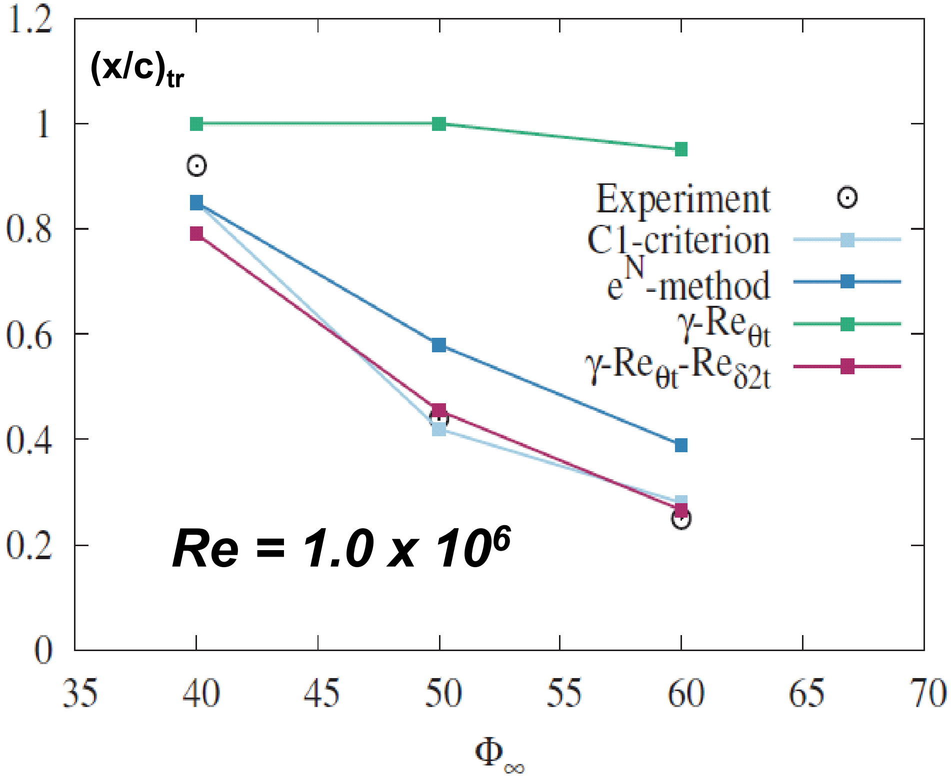

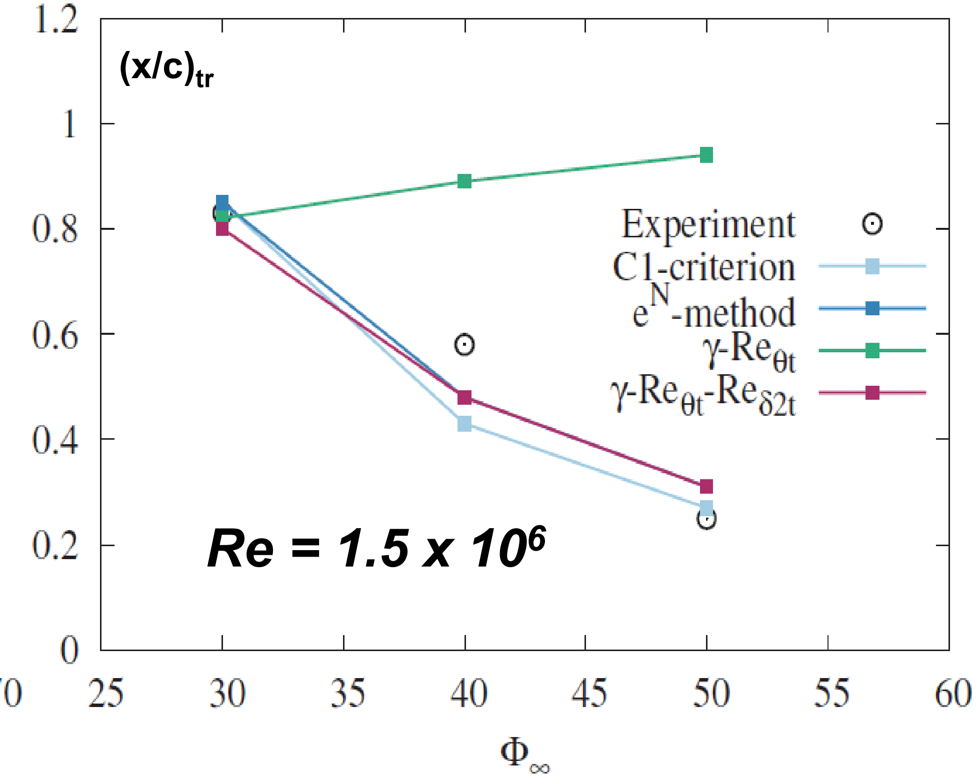

The γ-$Re_{\theta,t}$ Transport Equation Model
Extension to Three-dimensional Flows

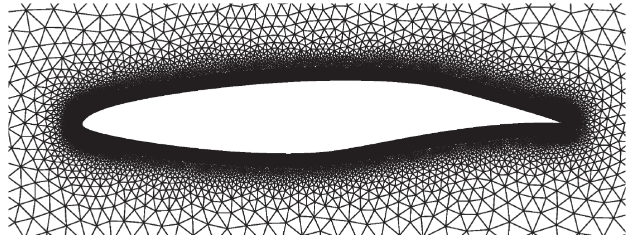

NLF(2)-0415 – infinite swept wing (2.5D)

- *Low M, Re = 1.93 x 10⁶ & 3.7 x 10⁶, α = -6°, Φ_∞ = 45°*
- *For Re > 2.3 × 10⁶, transition is dominated by CF instability*

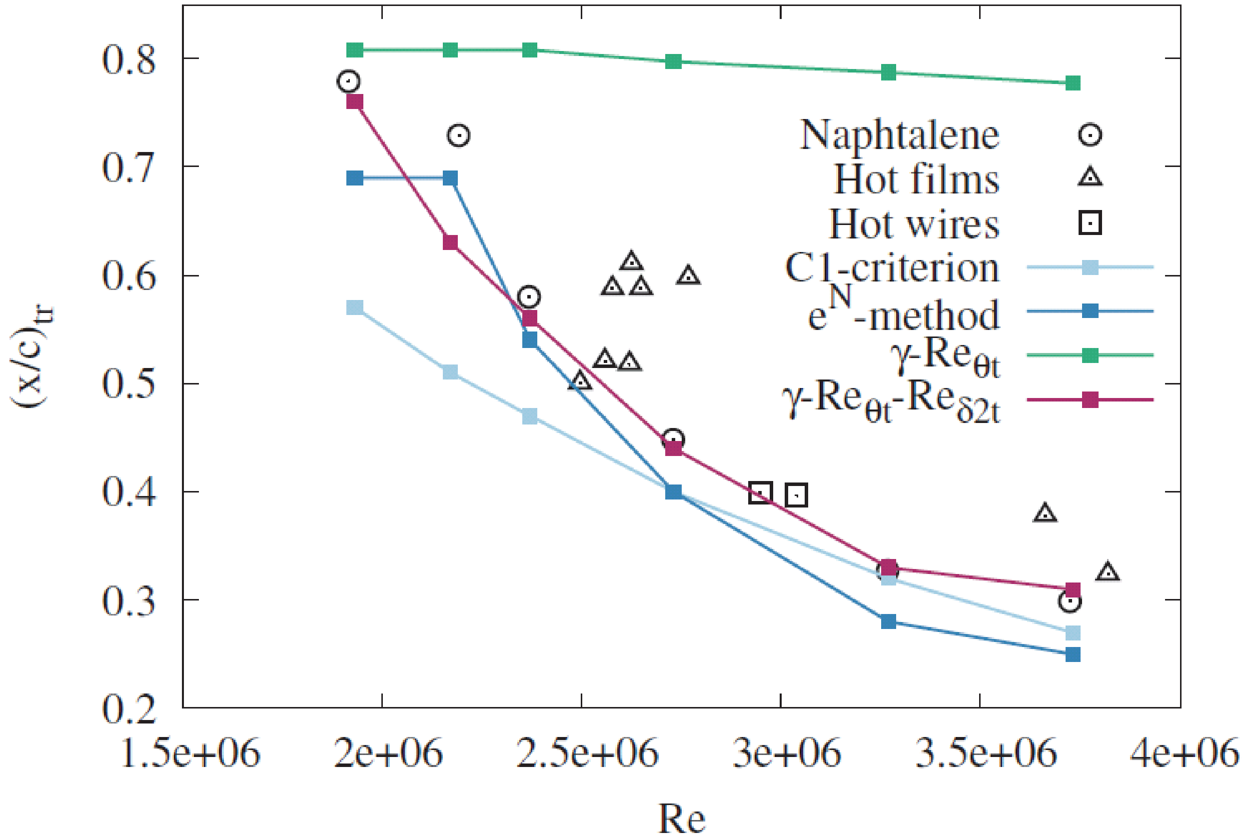

Conclusion
Transition Prediction in RANS-based CFD of External Flows

- Two transition prediction approaches for external flows of high potential have been presented
  - e^N method, evaluated along line-in-flight cuts or streamlines using different concepts of calculation of laminar boundary-layer data (1)
  - γ-$Re_{\theta,t}$ transport equation model (2)
- Both can be applied to general, complex geometries in parallel computation environments
  - (1) covering more transition mechanisms and a larger applicability range of the transition criteria
  - (2) offering more flexibility from a technical and practical application point of view
  - (1) yielding a high level of maturity and confidence in the method
  - (2) having a high potential of being a complementary method for extremely complex configurations in certain flow environments

Outlook
Transition Prediction in RANS-based CFD of External Flows

- (1) with streamline computation and RANS-based BL-data computation not yet push-button-technique for everyday use in industry, but an expert approach.
  - Industrialization has started currently.
- (2) is a rather new approach, still missing comprehensive experience and knowledge on the model behaviour in different situations (flow parameters, grid influence, settings of far-field BCs, numerical stability).
- γ-$Re_{\theta,t}$ approach has to be extended to
  - other turbulence models: mid term goal is coupling to RSMs
  - 3D transition mechanisms: CF started, ALT still to be tackled
- γ-$Re_{\theta,t}$-$Re_{\delta 2t}$ model to be tested on relevant 3D configurations
  - the ONERA M6 wing
  - the TELFONA (EU project) configurations tested in ETW
- γ-$Re_{\theta,t}$-$Re_{\delta 2t}$ model has to be calibrated to a wide range of flows.
- In aircraft aerodynamics at DLR, the γ-$Re_{\theta t}$ model only „survives“, if it is able to predict transition due to CF instabilities.